AN ABSTRACT OF THE THESIS OF

Purnima Subramaniam for the degree of Master of Science in Industrial Engineering presented on July 14, 2023.

Title: Multi-objective Optimization for Equitable Post-Disaster Relief Supply Distribution

Abstract approved: _____

Hector A. Vergara

Humanitarian logistics in the post-disaster phase of an earthquake requires detailed planning about the relief distribution network including assigning available distribution centers (DCs) to the affected areas, distribution of the relief commodities demanded by the affected population, and efficient allocation of the available vehicle fleet for the distribution in a short span of time. As the demand for relief commodities changes dynamically, the allocation of relief commodities requires a multi-period emergency plan to fully utilize the emergency resources efficiently. Furthermore, as a disaster occurs suddenly without any warning, relief supplies are insufficient in the initial phase of the disaster. At such times, the decision makers face difficulties distributing the available supplies equitably across all the affected areas without putting any particular community at risk.

This study focuses on two different dimensions: *efficiency* and *equity* by minimizing the total unmet demand as well as minimizing the total travel time to satisfy demand at different nodes across different time periods while requiring that the percentage of satisfied demand at

each node is within a specified deviation range from the average demand satisfaction rate for all nodes.

To address this problem, a deterministic multi-objective mathematical programming formulation is developed to model the design of a disaster relief distribution network with the primary objective of minimizing the total unmet demand across all demand nodes and the secondary objective of minimizing the total transportation time. The model is solved using the lexicographic method for a problem instance of a Cascadia Subduction Zone (CSZ) earthquake in the state of Oregon. Four scenarios are evaluated for two different earthquake magnitudes with different levels of damage to candidate DCs. Pareto optimal frontiers are obtained to determine the trade-off between the unmet demand and the total travel time for these scenarios. The model results show that an equitable distribution of relief commodities is possible at a relatively high demand satisfaction rate when supplies are still limited but the number of vehicles for two different modes of transportation is large. Moreover, shortages in vehicles significantly increase the unmet demand across different demand nodes. Overall, this research provides useful insights about the characteristics of the relief distribution network and provides a method for trade-off analysis that decision-makers can use to improve the efficiency of humanitarian logistics in a post-disaster setting.

Multi-objective Optimization for Equitable Post-Disaster Relief Supply Distribution

by

Purnima Subramaniam

A THESIS

submitted to

Oregon State University

in partial fulfillment of

the requirements for the

degree of

Master of Science

Presented July 14, 2023

Commencement June 2024

Master of Science thesis of Purnima Subramaniam presented on July14, 2023

APPROVED:

Major Professor, representing Industrial Engineering

Head of the School of Mechanical, Industrial and Manufacturing Engineering

---

Dean of the Graduate School

I understand that my thesis will become part of the permanent collection of Oregon State University libraries. My signature below authorizes release of my thesis to any reader upon request.

Purnima Subramaniam, Author

ACKNOWLEDGEMENTS

I would like to express my heartfelt gratitude to my advisor Dr. Hector A. Vergara for his support, guidance, and commitment throughout the entire process of this thesis. His expertise, insightful feedback, and encouragement played a crucial role in shaping this research. I am also grateful to my thesis committee members Dr. Joseph Agor, Dr. David Porter and Dr. Woodam Chung for their time and involvement in this research. Additionally, I would like to express my deepest gratitude to the Graduate School and the School of Mechanical, Industrial, and Manufacturing Engineering for honoring me with the Thesis Completion Award. This recognition is sincerely acknowledged.

Furthermore, I would like to express my deepest gratitude to my parents and my family for their constant love, support, and belief in my dreams. Their unyielding faith in me has been a driving force behind my accomplishments.

Last but not least, I am deeply grateful to my loving husband for his support and belief in my abilities. He has been my constant source of strength and my biggest cheerleader. His boundless encouragement and extraordinary support throughout this journey has been the cornerstone of my achievements. I dedicate my thesis to him.

TABLE OF CONTENTS

TABLE OF CONTENTS (continued)

Content Page

LIST OF FIGURES

Figure Page

LIST OF TABLES

Table Page

LIST OF APPENDIX TABLES

Table Page

1. Introduction

Natural disasters like earthquakes and tsunamis are largely unpredictable and cause severe damage to people, infrastructure and the economy. They leave behind lasting repercussions that take years to reverse. The Federal Emergency Management Agency (FEMA) has identified a National Risk Index for the United States that represents a community's relative risk for earthquakes when compared to the rest of the country (Figure 1). As shown in Figure 1, Oregon has a very high earthquake risk as it lies in the Cascadia Subduction Zone (CSZ), which has been identified as an active fault posing a major geological threat. It is anticipated that a major earthquake will occur in the Pacific Northwest (PNW) in the next 50 years (Oregon Resilience Plan, 2013).

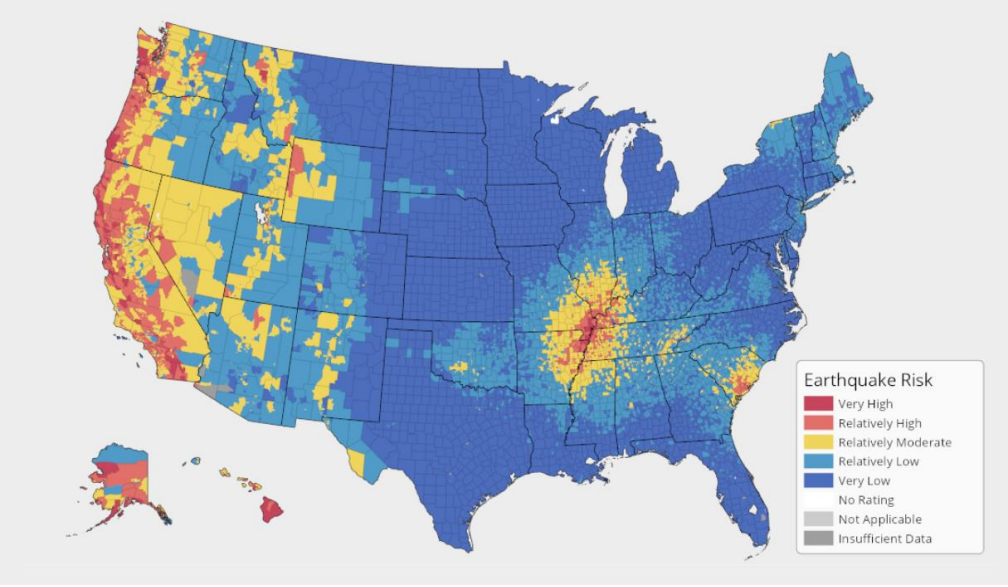

Source: https://hazards.fema.gov/nri/earthquake

Figure 1.1 *National Earthquake Risk Index*

In the immediate aftermath of a disaster, planning a quick and efficient response is vital to mitigate the destruction caused by the event (e.g., an earthquake and subsequent tsunami for a CSZ event). If executed efficiently and deployed promptly, a disaster recovery plan can

significantly reduce the destruction and fatality rate resulting from the event (Shravarani, 2019). The planning and execution of a disaster recovery plan is a daunting task as there are several challenges which must be addressed. Variability in demand, road conditions, and relief supplies have to be considered along with high level of coordination between rescue teams and government agencies in a short span of time and within an available budget. The immediate emergency response in the days following such disasters plays a key role in reducing the overall damage and destruction in the long run (Veysmoradia et al., 2017).

A disaster recovery plan includes two phases, a pre-event phase and a post-event phase. The pre-event phase deals with planning and preparation of activities in anticipation of a disaster such as allocating candidate distribution centers and relief shelters. The post-event phase or the response phase deals with the immediate response and recovery activities after the event, such as transportation and logistics for people and relief commodities. These decisions like allocating relief shelters for the survivors, relief distribution in the affected areas, the selection of the mode of transportation to be used for a specific region etc., have to be taken quickly and correctly (Altay et al, 2006). In the event of a high-magnitude earthquake, ground transportation is unreliable due to the potential severe damage to infrastructure resulting in road blockages and impassable routes (Veysmoradia et al., 2017). With the unpredictability of road conditions and the limited amount of time available in the response phase, air transportation like helicopters and unmanned aerial vehicles (UAVs) or drones would be very helpful to aid in immediate relief distribution of commodities like medicines and first aid kits, and to survey road conditions, casualties and potential survivors. Air transportation could also help to compensate shortages in the relief carrying capacity in emergency response systems by working in combination with other modes of transportation (Nedjati et al., 2015). Overall, using both aerial and ground transportation modes would minimize the travel time and increase route reliability for the distribution of relief supplies and the provision of emergency services.

At the same time, equity is an important aspect in disaster recovery planning that cannot be ignored. A disaster hit region has different requirements for relief goods to be supplied based on the population affected by the disaster. The areas where these requirements arise are usually called demand nodes. Sometimes decision makers face difficulties to make an ethical choice when supplies are insufficient to satisfy all demand nodes. With shortages of relief supplies, the distribution of emergency relief should be such that no particular community is at a higher risk to receive insufficient supplies and at the same time, it must be distributed to remote demand nodes in need, even if this compromises efficiency. This makes relief distribution a harder problem than regular commercial logistics problems (Liu et al., 2019).

This research will focus on multi-objective optimization of relief supplies distribution by using multiple modes of transportation (e.g., aerial and ground) while ensuring equitable relief distribution after an earthquake disaster. The proposed model will seek to make the relief distribution efficient by minimizing the total travel time for transporting different relief commodities while at the same time minimizing the total unmet demand for all demand nodes. The multi-objective optimization formulation is solved using the lexicographic approach. The lexicographic approach is a priority-based method to solve multi-objective optimization models, where the objective functions are solved in the order of their priority of importance (Volgenant, 2022). One advantage of using the lexicographic approach is that it helps the policy makers and decision makers to prioritize one objective over other, and in doing so, it avoids the conflicts that may arise by trying to balance multiple objectives. Since this study addresses strategic planning in the pre-disaster and post-disaster phases, a lexicographic approach was found to be the most suitable approach as decision makers will have the power to set priorities among multiple objectives and evaluate the resulting trade-offs between them. This study also aims to make the relief distribution fair, by ensuring that all affected people have equitable access to relief supplies.

The remainder of this thesis document is organized as follows. Section 2 reviews various research studies on humanitarian logistics and relief distribution in disasters. Section 3 describes the problem definition. Section 4 shows the details of the model description and mathematical formulation for the multi-objective optimization with equitable multi-period relief distribution. Section 5 presents the scenario generation methodology for computational testing and describes the model parameter estimation. Section 6 presents the computational results for the optimization problem and presents the sensitivity analysis for the model parameters. Finally, in Section 7, a discussion of the conclusions derived from the case study findings and the contribution of this research is presented along with some limitations and potential future research directions.

2. Literature Review

This study focuses on a multi-period integrated planning problem with strategic decisions about relief facility location in a pre-disaster stage, and tactical decisions on multi-commodity relief distribution using multiple modes of transportation in a post-disaster stage while ensuring an equitable distribution of relief supplies. In the rest of this section, related studies focusing on pre-disaster and post-disaster humanitarian logistics in this context are summarized and analyzed.

Humanitarian logistics has been extensively studied in recent years. The lack of proper logistical planning in the response phase of disaster management can lead to problems like poor accessibility and operation of relief facilities, inefficient use of vehicle fleets, and unavailability of appropriate transportation modes at the required time (Maghfirog and Hanaoka, 2020). Studies involving strategic decisions focus on the design of relief supply networks by defining plans for the location-allocation of distribution centers and relief shelters. Studies focusing on tactical and operational decisions put emphasis on post-disaster planning including inventory management, efficient allocation of vehicle fleets for relief distribution, transportation of relief distribution across multiple echelons of a relief supply network, generation of transportation routes for relief supply distribution, and the movement of injured people. Large-scale disasters often demand larger number of relief commodities in multiple affected areas simultaneously. The allocation of relief commodities is a continuous multi-period supply process and it takes multiple periods to meet the demands of relief commodities like food, water, and medicines (Wang et al., 2023). When demand and supply change dynamically in the initial stage of a disaster recovery phase, a multi-period emergency plan is necessary to fully utilize the emergency resources efficiently.

A well-developed strategic plan for relief facility location has a direct impact on operational costs and response times. It also ensures smooth and efficient operation of the rest of the disaster relief system (Shavarani, 2018). Decisions made in the pre-disaster phase influence the performance of the post-disaster or response phase. The location of a distribution center (DC) for relief supplies should be determined such that all potential demand nodes would be covered with the least number of DCs, and every potential demand node must be within a targeted response time in the relief network. Some studies like Condeixa et al. (2017) show how humanitarian logistics can benefit from risk management through pre-positioning of DCs and relief shelters to better attend the affected people in a disaster.

The severe damage to roads and infrastructure following a high magnitude disaster results in disruptions to the distribution network and uncertainty in road conditions. The limited amount of time for post-disaster relief operation makes it extremely difficult to identify and repair the damaged distribution network (Maghfirog and Hanaoka, 2020). In such cases, having multiple modes of transportation available for relief supply distribution helps to increase the performance of the system by increasing route reliability. Ghasemi et al. (2019) proposed a stochastic multi-objective, multicommodity flow with multi-modal transportation model using mixed integer mathematical programming with the objective of minimizing the location-allocation cost of the facilities and minimizing relief supply chain shortages. This paper solves a multi-vehicle problem (heterogenous vehicle fleet), but it does not consider the tradeoff between the different modes of transportation. Lui et al. (2019) presented a multi-modal location-routing problem to address shortages in relief supplies, road damages, and disaster severity. Aerial transportation (e.g., helicopter) is only considered for disconnected nodes. Otherwise, relief supply distribution is carried out via ground transportation. This paper focuses on vehicle routing and fair relief distribution only for a single time period and a single relief commodity. More recently, Maghfirog and Hanaoka (2020) formulated a single commodity,

multi-modal relief distribution network problem with time varying features in three-echelons, namely the supply node, the intermodal transfer node, and the demand node. Their objective function minimizes the delivery time and transportation costs. More recently, Gao et al. (2021) considered a bi-objective stochastic optimization model to transport relief commodities within a multi-modal transportation network with uncertain supply, demand, and road availability. Commodities are transported to demand nodes via helicopter when road blockages exist in certain routes. Most of the studies with multi-modal transportation focus on operational decisions like vehicle routing rather than on strategic decisions and lack a comprehensive multi-period, multi-commodity approach along with multi-modal transportation.

The use of drones in humanitarian logistics has spiked in recent years due to its various capabilities like autonomous maneuvering, identification of trapped survivors, and for urgent distribution of first aid and medicines. Nedjati et al. (2016) proposed the use of drones for rapid damage assessment of an affected region by capturing images from the site and creating a response map to extract useful information. Golabi (2017) considered the usage of drones for transporting relief commodities and proposed models to identify ideal drone launch locations and relief shelters. Drones were used for locations that cannot be reached by ground transportation or helicopters. Faiz et al. (2020) used two types of drones in their distribution network. A hotspot drone for identifying the demand of relief commodities and a delivery drone for delivering the commodities to people in need. Lu et al. (2022) proposed a truck-drone cooperative relief distribution model in which the drone is carried in the truck and both deliver relief commodities to demand nodes. The truck driver launches the drone from a launch point and the drone returns back to the same launch point after deliveries. Although recently drones are being considered in many research papers to deliver relief commodities in humanitarian logistics, in this study we consider only helicopters as the aerial mode of transportation.

Equity is also an important aspect in humanitarian logistics as it ensures equitable access to relief supplies and provides help to the people in need without discrimination. Equity can be temporal, where every demand is fulfilled within a certain time window. Equity can also be spatial where distribution in an area is considered. Or equity can be social, which is based on the extent to which demand is fulfilled in proportion to the need (Mahapatra and Mohanty, 2022; Karasu and Mortan, 2015). Sheu et al. (2006) considered a three-level relief distribution network in a post-earthquake area and developed a model to maximize the satisfaction of the people in the affected region by penalizing relief shortages. Cao et al. (2018) formulated a multi-stage, multi-commodity sustainable relief distribution problem with the objective of maximizing the lowest victims' perceived satisfaction (VPS) for all demand points using a genetic algorithm. Huang and Rafiei (2019) considered a multi-period relief distribution network and compared equity measures regarding delivery quantities, arrival times, and deprivation times in different locations. Lui et al. (2019) proposed a location–routing problem for relief distribution in the early post-earthquake stage with the aim to minimize the maximum and total loss of demand nodes and minimize the maximum time required for the demand node to receive relief supplies. Although, fairness and equity have been studied in the humanitarian logistics literature, there are few papers that include equity in a periodic location-allocation problem and analyze equity in a multi-period model (Arenas et al., 2019). According to Arenas at al. (2019), at the time of a supply shortage, partial delivery of relief supplies is always better than no delivery at all. Taking this into consideration, in our research, equity in resource allocation is achieved by a combination of minimizing the total unmet demand for all demand nodes and restricting the difference in the percentage of demand satisfaction between all demand nodes in a given time period. Although minor deviations are permissible, this model is formulated such that the deviation in the demand satisfaction rate falls within a predefined range. With this constraint, every demand node receives a similar fraction of their demand,

rather than fully satisfying the demand at some demand nodes while leaving other demand nodes unattended. This ensures that even at the time of relief shortages, no particular community is at a higher risk of disadvantage than others.

In the existing literature, very few papers have included the equity aspect in their modeling. The studies that include equity, either lack a multi-modal approach or a multi-period approach. Ghasemi et al., (2019) explored a multi-objective, multi-commodity, multi-period, and multi-vehicle problem with the objective of minimizing the total cost of the location-allocation of facilities and minimizing the amount of the shortage of relief supplies. This paper lacks an equity aspect and does not take multi-modal transportation into account. Tzeng et al. (2007) considers a multi-objective optimization problem with efficiency and fairness pursuits, but this paper considers only a single mode of transportation. Gao et al. (2021) adopted a dual objective optimization for maximizing fairness and minimizing the maximum transportation time in a multi-modal network flow problem, but only considered the problem for a single period. Wang et al. (2023) considered a three-dimensional humanitarian problem with focus on effectiveness, efficiency and equity, but it does not consider a multi modal approach.

Furthermore, most of the current studies have considered a single objective optimization problem. The most frequent objectives pursued by these studies are cost minimization and travel time minimization. The existing research in the areas mentioned above for disaster recovery planning are largely contained within isolated pockets. Most of the research focuses on using multi-modal transportation in multiple echelons, where each echelon has a pre-defined mode of transportation and very few papers focus on equitable resource allocation in multiple periods. The decision between aerial or ground transportation requires a tradeoff between transportation time and total transportation cost. The current literature lacks a comprehensive, integrated approach that includes a multi-commodity, multi-period

distribution network using multiple modes of transportation simultaneously at the time of a disaster.

The contributions of this study based on the gaps identified in the current literature review are as follows: First, most of the multi-objective research in the field of humanitarian logistics of relief supplies location-allocation rarely consider an equity perspective. This study focuses on the humanitarian logistics objectives in two different dimensions: efficiency and equity by minimizing the total travel time as well as minimizing the total unmet demand in all demand nodes across all periods. Furthermore, based on the intensity of relief shortages at the time of the disaster, this research will aid the policy makers to optimize the relief distribution by restricting the deviation in the demand satisfaction rate within a predefined range. This will ensure that at the time of relief shortages, no particular community is at a higher risk of disadvantage than others. Second, most of the current literature focuses on single-period relief distribution in humanitarian logistics which does not consider the dynamic fluctuations in the relief supply and demand quantities as time passes by after the occurrence of the disaster event. This paper simultaneously minimizes the total travel time and the unmet demand of multiple commodities across multiple periods, which will help policy makers when planning the supply distribution strategy. And finally, to the best of our knowledge, no previous contribution has considered a bi-objective optimization problem in humanitarian logistics with multi-commodity, multi-modal, and multi-period facility location-allocation with an equity perspective in a multiple DC to multiple demand node network. This research will deal with the planning and deployment of multi-modal transportation for the efficient flow of commodities from DCs to demand nodes to meet the urgent requirement of affected people using limited resources available at the time of a disaster. It will be applied taking into consideration the variation in travel times, supply, and demand parameters based on multiple

scenarios of a CSZ earthquake. Table 2.1 summarizes the relevant literature reviewed and discussed in this section and positions our current research.

Table 2.1 *Summary of Relevant Literature*

Article	Year	Objective	Period	Mode	Commodity	Equity
Barbarosoglu and Arda	2004	Single	Single	Multi	Multi	No
Tzeng et al.	2007	Multi	Multi	Single	Multi	No
Afshar and Haghani	2012	Single	Multi	Single	Multi	Yes
Huang et al.	2015	Multi	Single	Single	Single	Yes
Ransikarbum and Mason	2016	Multi	Single	Single	N/A	Yes
Noyan and Kahvecioglu	2017	Multi	Single	Single	Single	Yes
Cao et al.	2017	Multi	Multi	Single	Multi	Yes
Condeixa et al.	2017	Single	Single	Single	Multi	No
Huang and Rafiei	2019	Multi	Multi	Single	Single	Yes
Liu et al.	2019	Multi	Single	Multi	Single	Yes
Ghasemi et al.	2019	Multi	Multi	Single	Multi	No
Mohammadi et al.	2020	Multi	Multi	Single	Multi	Yes
Maghfiroh et al.	2020	Single	Multi	Multi	Single	No
Ershadi and Shemirani	2020	Multi	Multi	Single	N/A	Yes
Hernandez-Leandro et al.	2022	Multi	Single	Single	Multi	Yes
Mahapatra and Mahanty	2022	Single	Single	Single	N/A	Yes
Wang and Sun	2023	Multi	Multi	Single	Multi	Yes
This Research	***2023***	***Multi***	***Multi***	***Multi***	***Multi***	***Yes***

3. Problem Definition

The initial phase after the onset of an earthquake is a critical phase where multiple decisions must be made within a short span of time regarding which candidate distribution centers (DCs) will be used for distributing relief supplies to affected areas, what modes of transportation to use, what routes to use, etc. As it is not possible to predict the exact magnitude and timing of an earthquake, it is difficult to forecast the actual damages to transportation networks like roads, airports, and seaports, the number of people affected, the damages to buildings and infrastructure, and the demand for relief commodities in the days following the disaster. In the aftermath of an earthquake, transportation capacity, availability of particular modes of transportation, availability of emergency resources and relief supplies are always scarce (Maghfirog and Hanaoka, 2020). These uncertainties make it challenging to plan and execute post-disaster humanitarian logistics activities like relief distribution, movement of people to shelters, etc. Timely and efficient decisions in the post-disaster phase are vital as it can help to bring life back to normalcy faster and can minimize the suffering of the affected people. A robust yet flexible relief distribution plan can help support decision making, the selection of suitable modes of transportation, and can facilitate making the relief distribution equitable across the affected population.

After a disaster occurs, relief commodities are demanded in large quantities from multiple affected areas. A decision regarding the assignment of limited DCs to the various demand nodes can make the process efficient and smoother. Disasters like earthquakes also result in the inability to access various modes of transportation like ground and air transportation due to damage to the transportation infrastructure. A detailed plan for relief distribution with multiple modes of transportation is imperative for efficient distribution of relief supplies. This research addresses the problem of determining which mode of transportation to use when distributing relief commodities from an assigned DC to demand

nodes. The problem also requires determining the amount of relief commodities to be sent on a particular mode of transportation on a given period after the disaster occurs such that total unmet demand across all demand nodes is minimized. By considering the demand and supply of relief commodities over multiple time periods, this study is able to capture the variations and dynamic fluctuations in the demand and supply of relief commodities in the aftermath of an earthquake.

A disaster displaces people from their homes and can cause immense physical and psychological distress to the affected population. Unfair relief distribution and putting certain communities at a higher risk of disadvantage can further aggravate the distress of the affected people. The problem under study also considers ensuring an equitable relief distribution across different demand nodes in case of supply shortages. In this context, equity in resource allocation is achieved by combining the minimization of the total unmet demand for all commodities, across all demand nodes on all periods, and restricting the difference between the actual demand satisfaction rate for individual demand nodes and the average demand satisfaction rate for all demand nodes in a given time period.

In this research, we focus on the trade-offs between the total unmet demand and the total travel time to distribute relief supplies. The goal is to provide decision makers with solutions which are optimal in both quantity of demand met and timely response. In a post-disaster response phase, cost-based decisions might not be the best approach to adopt. Rather than focusing on minimizing the cost of the entire relief operation, this research considers a fixed budget for the opening DCs and the transportation costs associated with the relief operations.

To summarize, given a relief network with candidate DCs and multiple demand nodes, this research problem requires determining: (1) the location of DCs for pre-positioning supplies, (2) the assignment of DCs to various demand nodes, (3) the amount of each relief

commodity to be delivered from each DC to demand nodes considering equitable distribution on each period post-disaster, (4) the mode of transportation (ground or aerial) to be used to make these deliveries, (5) the actual demand satisfaction rate of each commodity for every demand node for every period, and (6) the average demand satisfaction rate for every commodity in a given time period. The goals are minimizing the overall unmet demand at the same time as minimizing the time to deliver the relief supplies across all periods after the disaster. Figure 3.1 shows the relief supply distribution network under study. The relief distribution network in Figure 3.1 comprises of candidate DCs denoted by squares, and multiple demand nodes denoted by cubes. The relief commodities are supplied from the DCs to each of the demand nodes either by trucks (i.e., ground transportation), helicopters (i.e., air transportation), or both in each period.

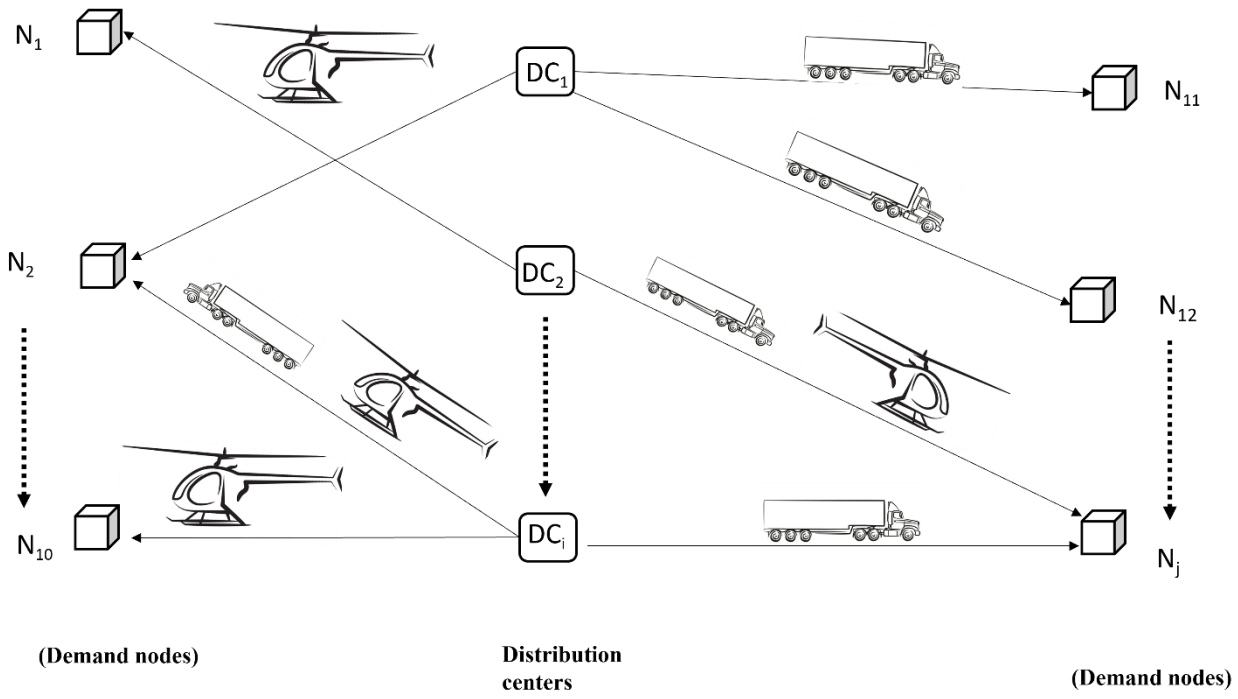

Figure 3.1 *Relief Supply Distribution Network*

The following assumptions are considered for developing a mathematical programming model of the problem under study:

1. The location of all candidate DCs and demand nodes are known.
2. A DC can supply multiple demand nodes and a demand node can be supplied by multiple DCs.
3. The demand and supply for all relief commodities in each period are known.
4. Shortages in supply are allowed. Backorders for the relief commodities are not considered.
5. The number of homogeneous vehicles for ground transportation and air transportation modes are known.
6. A time period can be set for multiples of days or multiples of 24 hours. In this study, we consider a planning horizon with three time periods, where each time period is set to be a window of two days or 48 hours.
7. Multiple modes of transportation can serve each demand node.
8. The time required to travel between a DC and a demand node in a given time period is known.
9. The cost associated with opening a DC and the unit cost of flow transportation via ground and air between all DC and demand nodes are known.
10. The unmet demand for a commodity is calculated at every demand node for every period.

To the best of our knowledge, a multi-objective optimization problem with a combination of all the above features and assumptions has not been presented before (see Table 2.1). In Chapter 4, we present a mathematical formulation to solve this problem.

4. Model Formulation and Solution Method

This chapter includes the notation for sets, parameters, and decision variables used in a multi-objective optimization mathematical programming formulation for the problem described in Chapter 3. It also includes a detailed description of the objective functions and the constraints used in the formulation. And finally, a description of the solution approach for solving this multi-objective optimization problem and its implementation are presented.

4.1 Notation

Sets

K = Set of relief commodities k,
I = Set of distribution centers (DCs) i,
J = Set of demand nodes j,
P = Set of time periods p.

Parameters

C_i = fixed cost associated with opening a DC i,

C_{ij}^{kg} = unit cost of flow of commodity k from DC i to demand node j via ground,

C_{ij}^{ka} = unit cost of flow of commodity k from DC i to demand node j via air,

$t_{ij}^{g(p)}$ = expected time to transport commodity k from DC i to demand node j via ground in time period p,

$t_{ij}^{a(p)}$= expected time to transport commodity k from DC i to demand node j via air in time period p,

$s_i^{k(p)}$= supply of commodity k at DC i in time period p (in pounds),

$d_j^{k(p)}$= demand of commodity k at demand node j in time period p (in pounds),

V_g = total number of available ground transportation vehicles,

V_a = total number of available air transportation vehicles,

L_g = loading capacity of a ground transportation vehicle (in pounds),

L_a = loading capacity of an air transportation vehicle (in pounds),

Δ = minimum percentage of demand satisfaction rate for a demand node,

δ = deviation allowed in demand satisfaction rate for demand nodes,

B = available budget.

Decision Variables

$x_i =$ 1 if DC i is open

0 otherwise,

$y_{ij}^{kg(p)}$ = 1 if demand for commodity k at node j is served by DC i via ground in time period p

0 otherwise,

$y_{ij}^{ka(p)}$ = 1 if demand for commodity k at node j is served by DC i via ground in time period p

0 otherwise,

$z_{ij}^{kg(p)}$ = amount (in pounds) of commodity k delivered from DC i to demand node j via ground in time period p,

$z_{ij}^{ka(p)}$ = amount (in pounds) of commodity k delivered from DC i to demand node j via air in time period p,

$r_j^{k(p)}$ = demand satisfaction rate for commodity k at demand node j in time period p,

$\hat{r}^{k(p)}$ = average demand satisfaction rate for commodity k in time period p,

$u_j^{k(p)}$ = unmet demand (in pounds) of commodity k at demand node j in time period p.

4.2 Multi-objective Mathematical Formulation

A multi-objective mixed-integer programming formulation for the problem defined in Chapter 3 is introduced below.

$$Minimize\ f_1 = \sum_{j \in J} \sum_{k \in K} \sum_{p \in P} u_j^{k(p)} \tag{1}$$

$$Minimize\ f_2 = \sum_{i\in I}\sum_{j\in J}\sum_{k\in K}\sum_{p\in P}\left(t_{ij}^{g(p)}y_{ij}^{kg(p)} + t_{ij}^{a(p)}y_{ij}^{ka(p)}\right) \tag{2}$$

Subject to:

$$\sum_{i\in I}\left(y_{ij}^{kg(p)} + y_{ij}^{ka(p)}\right) \geq 1, \qquad \forall j \in J, \forall k \in K, \forall p \in P \tag{3}$$

$$\sum_{j\in J}\left(z_{ij}^{kg(p)} + z_{ij}^{ka(p)}\right) \leq s_i^{k(p)}, \qquad \forall i \in I, \forall k \in K, \forall p \in P \tag{4}$$

$$\sum_{i\in I}\left(z_{ij}^{kg(p)} + z_{ij}^{ka(p)}\right) \geq \Delta d_j^{k(p)}, \qquad \forall j \in J, \forall k \in K, \forall p \in P \tag{5}$$

$$r_j^{k(p)} = \sum_{i\in I}\left(z_{ij}^{kg(p)} + z_{ij}^{ka(p)}\right)/d_j^{k(p)}, \qquad \forall j \in J, \forall k \in K, \forall p \in P \tag{6}$$

$$\hat{r}^{k(p)} = \sum_{j\in J} r_j^{k(p)}/|J|, \qquad \forall k \in K, \forall p \in P \tag{7}$$

$$r_j^{k(p)} - \hat{r}^{k(p)} \leq \delta, \qquad \forall j \in J, \forall k \in K, \forall p \in P \tag{8}$$

$$-r_j^{k(p)} + \hat{r}^{k(p)} \leq \delta, \qquad \forall j \in J, \forall k \in K, \forall p \in P \tag{9}$$

$$u_j^{k(p)} = d_j^{k(p)} - \sum_{i\in I}\left(z_{ij}^{kg(p)} + z_{ij}^{ka(p)}\right), \qquad \forall j \in J, \forall k \in K, \forall p \in P \tag{10}$$

$$y_{ij}^{kg(p)} \leq |J|x_i, \qquad \forall i \in I, \forall j \in J, \forall k \in K, \forall p \in P \tag{11}$$

$$y_{ij}^{ka(p)} \leq |J|x_i, \qquad \forall i \in I, \forall j \in J, \forall k \in K, \forall p \in P \tag{12}$$

$$z_{ij}^{kg(p)} \leq d_j^{k(p)}y_{ij}^{kg(p)}, \qquad \forall i \in I, \forall j \in J, \forall k \in K, \forall p \in P \tag{13}$$

$$z_{ij}^{ka(p)} \leq d_j^{k(p)}y_{ij}^{ka(p)}, \qquad \forall i \in I, \forall j \in J, \forall k \in K, \forall p \in P \tag{14}$$

$$\sum_{k\in K} z_{ij}^{kg(p)} \leq L_g, \qquad \forall i \in I, \forall j \in J, \forall k \in K, \forall p \in P \tag{15}$$

$$\sum_{k\in K} z_{ij}^{ka(p)} \le L_a, \qquad \forall i \in I, \forall j \in J, \forall k \in K, \forall p \in P \tag{16}$$

$$\sum_{i\in I}\sum_{j\in J}\sum_{k\in K} z_{ij}^{kg(p)} \le V_g L_g, \qquad \forall p \in P \tag{17}$$

$$\sum_{i\in I}\sum_{j\in J}\sum_{k\in K} z_{ij}^{ka(p)} \le V_a L_a, \qquad \forall p \in P \tag{18}$$

$$\sum_{i\in I} C_i x_i + \sum_{i\in I}\sum_{j\in J}\sum_{k\in K}\sum_{p\in P} C_{ij}^{kg}\, z_{ij}^{kg(p)} + \sum_{i\in I}\sum_{j\in J}\sum_{k\in K}\sum_{p\in P} C_{ij}^{ka}\, z_{ij}^{ka(p)} \le B \tag{19}$$

$$x_i \in \{0,1\} \quad \forall i \in I \tag{20}$$

$$y_{ij}^{kg(p)} \in \{0,1\} \quad \forall i \in I, \forall j \in J, \forall k \in K, \forall p \in P \tag{21}$$

$$y_{ij}^{ka(p)} \in \{0,1\} \quad \forall i \in I, \forall j \in J, \forall k \in K, \forall p \in P \tag{22}$$

$$z_{ij}^{kg(p)} \ge 0 \qquad \forall i \in I, \forall j \in J, \forall k \in K, \forall p \in P \tag{23}$$

$$z_{ij}^{ka(p)} \ge 0 \qquad \forall i \in I, \forall j \in J, \forall k \in K, \forall p \in P \tag{24}$$

$$r_j^{k(p)} \ge 0 \qquad \forall j \in J, \forall k \in K, \forall p \in P \tag{25}$$

$$\hat{r}^{k(p)} \ge 0 \qquad \forall k \in K, \forall p \in P \tag{26}$$

$$u_j^{k(p)} \ge 0 \quad \forall j \in J, \forall k \in K, \forall p \in P \tag{27}$$

4.2.1 Objective Functions

Equation (1) and Equation (2) are the objective functions. Equation (1) minimizes the total unmet demand for all commodities for all demand nodes across all time periods. Equation (2) minimizes the total travel time for all commodities from DCs to demand nodes across all time periods. We assume that demand comes from people displaced from their homes and requiring temporary shelter. A delay in receiving relief commodities for displaced people is definitely not desirable, but it would not necessarily be as critical as having the ability to eventually distribute more relief to more people in need. For this reason, this model prioritizes minimizing

the total unmet demand for all relief commodities in all demand nodes across all time periods over minimizing the total travel time. Furthermore, the unmet demand is an indicator used to measure the quality of service of humanitarian relief logistics systems (Wang and Sun, 2023). By minimizing the total unmet demand and the total travel time in all time periods, this model aims to maximize the efficiency and effectiveness (i.e., improve the overall quality) of the disaster response logistics system. In addition, with a bi-objective mathematical formulation, the model also allows the decision makers to consider trade-offs between unmet demand and travel time minimization. This makes the model more flexible and adaptable for multiple situations.

4.2.2 Constraints

Equation (3) ensures that each demand node is served by at least one DC for every commodity in every time period via air or ground. Equation (4) ensures that the allocated amount of commodity *k* for all demand nodes in every time period is less than or equal to the total supply of commodity *k* at every DC *i* in every time period. Equation (5) requires that the minimum demand satisfaction rate (Δ) be met at every demand node *j* for every commodity *k* in every time period *p*. Equation (6) calculates the actual demand satisfaction rate at each demand node *j* for every commodity *k* in every time period *p*. Equation (7) calculates the average demand satisfaction rate for all demand nodes for every commodity *k* in every time period *p*. Equation (8) and Equation (9) specify that the deviation of demand satisfaction rate for every commodity *k* at a demand node *j* should be within δ percent of the average demand satisfaction rate for all nodes in every time period *p*. Equation (10) calculates the unmet demand for each commodity *k* at each demand node *j* in each time period *p*. Equation (11) and Equation (12) ensure that the demand nodes are assigned to be served only from established DCs in every time period *p* via ground and air, respectively. Equation (13) and Equation (14) ensure that the commodities flow only via established connections in every time period *p* via ground and air, respectively.

Equation (15) and Equation (16) limit the amount (in pounds) of commodities to be carried by air and ground transportation in a single trip between an established DC and a demand node in a time period to their respective loading capacities for the two modes of transportation. Equation (17) and Equation (18) ensure that the total weight amount of relief carried by air and ground transportation in every time period does not exceed the total capacity provided by the vehicles available for the two modes of transportation. Equation (19) is a budget constraint for the entire operation considering the fixed cost associated with opening DCs and the cost of flowing commodities from DCs to demand nodes via ground and air. Finally, Equations (20)-(27) are variable type constraints.

4.3 Solution Approach

The proposed multi-objective optimization model is solved using the lexicographic method (Rao, 2009). In the lexicographic method, the objective functions are ranked in order of their priority or importance and solved one at a time. Consider the multi-objective optimization problem shown below with *i* objectives (Rao, 2009):

$$Minimize\ f_i(X) \tag{28}$$

$$\text{Subject to:} \quad f_j(X) = f_j^*, \qquad j = 1,2,\dots,i-1 \tag{29}$$

$$g_k(X) \leq 0, \qquad k = 1,2,\dots,\text{n} \tag{30}$$

For the bi-objective optimization problem shown in Equations 28 to 30, the objective function with highest priority $f_1(X)$ is minimized first to obtain the minimum value of the first objective function $f_1 = f_1(X^*)$ where X^* is an optimal solution. After minimizing the first objective, the method tries to find the minimum value for the subsequent objective $f_2(X)$ with a priority of rank of 2 subject to the additional constraint that the value of the first objective

function must be equal to its optimal value. The constraint set for the multi-objective problem $g_k(X)$ remains the same for both of the objective functions.

In the proposed multi-objective optimization problem, the first objective, which is the total unmet demand, is minimized first to obtain the minimum f_1^*. The solution X^* at this stage in the optimization problem corresponds to the optimal solution for a single objective optimization problem that minimizes the total unmet demand without considering the total travel time in the supply distribution network. The method then minimizes the second objective function $f_2(X)$, which is the total travel time, while maintaining the total minimized unmet demand from the first objective.

Finally, an optimal Pareto front is obtained with a set of non-dominated solutions, which are feasible solutions not dominated by any other solutions such that an improvement in any one objective is only possible at the expense of a worse solution in at least one other objective. An optimal Pareto front is generated by increasing the relative tolerance of the unmet demand (i.e., the first objective function), until no improvement in the total travel time (i.e., the second objective function) can be gained.

4.4 Solution Method Implementation

The mathematical formulation and its solution method were implemented using Python 3.9. Solutions were obtained using Gurobi 9.5.2 on a machine with Intel® CoreTM i5 CPU, 2.50 GHz and 16 GB of RAM.

To verify the functionality and validate the performance of the proposed model and solution method, we generated a test data set for a small network comprising of two distribution centers (DCs) and five demand nodes with a trivial solution for a simplified version of the problem without the equity constraints and an unlimited number of vehicles available. A solution for this small network instance was obtained through manual optimization minimizing

the transportation time by allocating the nearest demand nodes to the DCs and minimizing the unmet demand by distributing all of the available supply at the DCs. Subsequently, the same instance was solved using the model implemented in Python and solved with Gurobi. No errors were encountered during the process verifying the functionality of the implemented model. Furthermore, the results obtained with the implemented model were then validated by comparing them with the optimal solution found manually. By comparing the results, it was confirmed that the implemented model produced consistent and accurate outcomes, thereby validating the implemented model for this small network instance.

5. Scenario Generation for Computational Testing

This section contains a description about the approach used to generate different earthquake scenarios for the application of the proposed model and solution model, and explains how the values of different model parameters were estimated for computational testing.

The proposed disaster relief multi-objective optimization model is tested with a case study for a Cascadia Subduction Zone (CSZ) earthquake event in the state of Oregon (Buylova et al., 2020). The Oregon Department of Emergency Management (OEM) predicts that there is a 37% chance of a CSZ megathrust earthquake in the Pacific Northwest region, with a magnitude of 7.1 and above, in the next 50 years (Oregon.gov).

To generate earthquake scenarios for a CSZ event and collect data for model parameters, we used Hazus-MH, a GIS-based natural hazard loss estimation software developed by the Federal Emergency Management Agency (FEMA) (fema.gov), along with ShakeMaps developed by the US Geological Survey (USGS) (earthquake.usgs.gov/data/shakemaps). ShakeMaps simulates scenarios based on the specified magnitude for an earthquake at a fault line from those provided by the National Earthquake Information Center (NEIC) database and estimates the social and economic damage that comes with it. With ShakeMaps, a spatial representation of an earthquake scenario along with shaking intensity and ground motion can be generated. In this study, the Cascadia megathrust fault line was selected to generate an earthquake scenario with a depth of 21m and an epicenter located at 45.061°N, 124.418°W denoted by the yellow mark in Figure 5.1. After generating a disaster scenario with a specific magnitude, the predicted damage and loss data were obtained for the study region of Oregon to generate an instance of the proposed mathematical model for solution.

Hazus-MH estimates the social impact of the hazard in terms of the number of people displaced from their homes due to an earthquake, number of people seeking temporary public shelters and the estimate of casualties, that is, the number of people who will be injured and killed by the earthquake. The casualties are broken down into four severity categories that describe the extent of the injuries, from Level 1 being the least severe to Level 4 being the most severe. Two different magnitudes for a CSZ earthquake were considered: M9.3 and M8.0. Hazus-MH estimates a total economic loss for the M9.3 earthquake to be 311,325.40 (millions of dollars) and 295,065.35 (millions of dollars) for an earthquake of magnitude M8.0. These cost estimates include the building, transportation and utility related losses based on the region's general building type and transportation lines (usgs.gov/shakemap).

The Hazus-MH software provides a contour map specifying the intensity of ground shaking and the magnitude of damage after an earthquake. Figure 5.1 shows a contour map for the state of Oregon for the M9.3 CSZ earthquake event. The contour map uses the scale presented in Figure 5.2 to estimate the intensity of the earthquake. According to Hazus-MH, the regions with an earthquake intensity of VI and above (i.e., orange and red regions) will experience strong to extreme shaking and moderate to very heavy damage. Regions with intensity V and below will experience moderate ground shaking and have damage ranging from none to light.

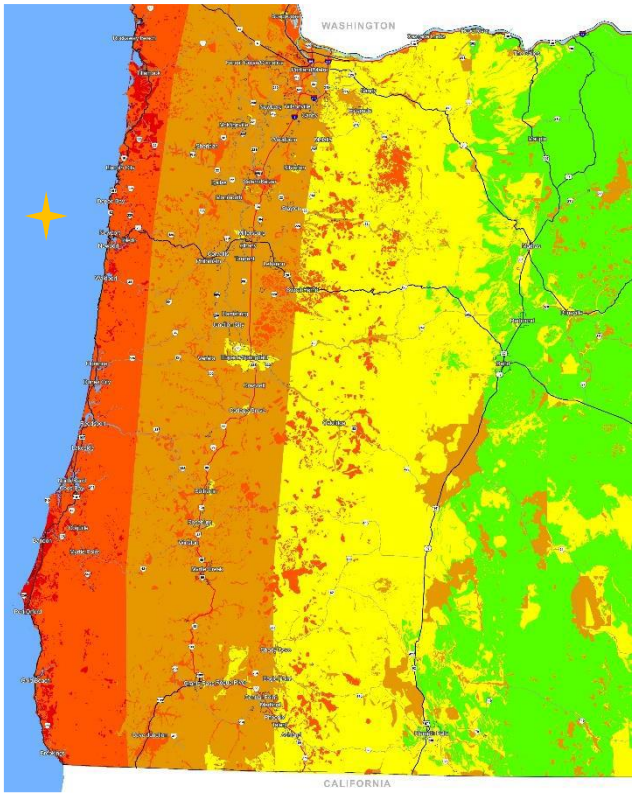

Figure5.1 *CSZ Earthquake Contour Map for Earthquake Damage*

Shaking	Not felt	Weak	Light	Moderate	Strong	Very Strong	Severe	Violent	Extreme
Damage	none	none	none	Very Light	Light	Moderate	Heavy	Heavy	Very Heavy
Intensity	I	II-III	IV	V	VI	VII	VIII	IX	X+
Scaling Factor	1	1	1	1	4	5	6	7	8

Source : https://www.usgs.gov/media/images/modified-mercalli-intensity-scale

Figure 5.2 *Hazus-MH Scale for Earthquake Damage*

5.1 Earthquake Scenarios

Natural disasters like earthquakes pose a serious threat to humankind due to the fact that they occur without any warming and leave no time for people to react to it. The destruction caused in the aftermath of an earthquake depends on various factors like its magnitude, the intensity of its occurrence, the time of occurrence etc. While scientists have made significant progress in understanding the mechanism of earthquakes and detecting their occurrences, there is still

no reliable method to predict the magnitude and the potential damage that they can cause (Galkina and Grafeeva, 2019). The potential CSZ earthquake in Oregon is predicted to have a magnitude ranging between M7.1 and M9.3 according to the Oregon Department of Emergency Management (oregon.gov/oem). To account for this uncertainty in the disaster planning stage, it is important to consider a range of possible scenarios. The result from multiple scenarios can be used to develop appropriate response plans that consider the potential impact of earthquakes of varying magnitudes. We vary the magnitude of the CSZ earthquake and the availability of candidate DCs to create four different scenarios for a CSZ earthquake event, as shown in Figure 5.3.

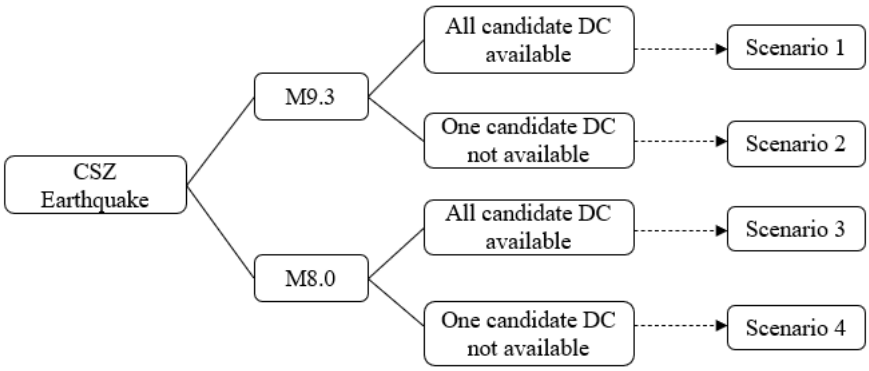

Figure 5.3 *CSZ Earthquake Scenarios*

In this study, we use the magnitudes of M8.0 and M9.3 to create CSZ earthquake scenarios using ShakeMaps. Analyzing multiple scenarios improves our awareness and assessment of the potential damages from the disaster event and is essential to improve overall disaster preparedness. By using ShakeMaps, we generate scenarios based on realistic data as every simulation takes into consideration shaking intensity, soil maps, ground motion and other related factors that are specific for the Cascadia Subduction Zone fault.

Additionally, since the exact amount of damage caused by any earthquake is impossible to predict, we consider two possibilities for each earthquake scenario: one with all candidate

DCs being available and functional, and one in which one of the candidate DCs is not available (i.e., DC is damaged). By doing this, we are modifying the availability of the supply of different relief commodities. Analyzing the results from the different scenarios allows us to seek a better understanding of the performance of the proposed formulation and develop insights to aid in the planning for uncertain future scenarios minimizing the potential impact of these events and ensuring a more effective disaster response.

5.2 Case Study Model Parameter Estimation

The Hazus-MH software provides an estimate of social losses including displaced households, people requiring temporary shelters, and casualties for each county. The CSZ earthquake damage contour map and the estimates of the affected population in each county obtained from Hazus-MH are used to assign the location of demand nodes and DCs for our case study. The DCs are assumed to be large temporary storage spaces from where the relief supplies will be distributed to different demand nodes. The demand nodes act as the first point of relief collection from the DCs for the affected counties and nearby local towns. Depending on the post-earthquake damages and the operations of the relief organization, the relief supplies delivered to demand nodes can be further distributed by vehicles to local beneficiaries within the county or alternatively people in the affected region can travel to these demand nodes to receive relief supplies. However, in this study, we do not consider the further distribution of relief from the demand nodes.

As the majority of the destruction and heavy damage due to the CSZ earthquake would occur along the Oregon Coast according to the contour map in Figure 5.1 with an intensity of VIII or higher as estimated by Hazus-MH, all the candidate DCs are identified in regions with an intensity of VII or lower. The yellow and green regions in the contour map in Figure 5.1 suggest that these places would experience moderate to light shaking, hence these regions do

not have any demand nodes and all demand nodes are concentrated on the red and orange damage bands. Six major cities with a population of at least 10,000 people or higher in these regions were selected and the centroids of these cities were chosen for the placement of the candidate DCs. Based on the damage estimated by Hazus-MH, the demand nodes are placed in counties with the maximum number of displaced people. Fourteen cities within each of those counties were selected and the centroids of these cities were chosen for the placement of the demand nodes. Figure 5.4 shows the placement of the candidate DCs (green crosses) and the demand nodes (red dots) that are established for this case study.

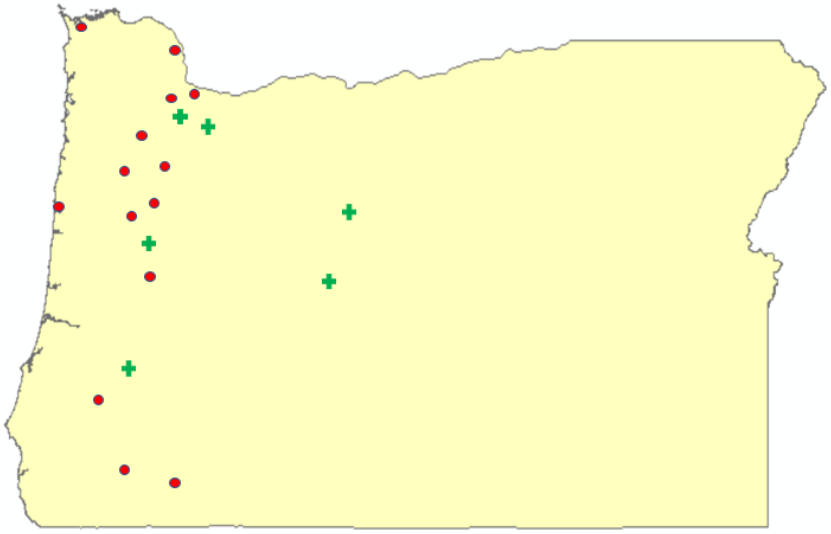

Figure 5.4 *Relief Distribution Network in the State of Oregon.*

Table 5.1 lists the candidate DCs represented by green crosses in Figure 5.4. Table 5.2 lists the demand nodes used in the case study, represented by the red dots in Figure 5.4.

Table 5.1 *List of Candidate DCs*

ID	Candidate DC
1	Sandy
2	Oregon City
3	Roseburg
4	Madras
5	Bend
6	Junction City

Table 5.2 *List of Demand Nodes*

ID	Demand Node
1	Beaverton
2	Portland
3	Astoria
4	St. Helens
5	McMinnville
6	Salem
7	Dallas
8	Newport
9	Albany
10	Corvallis
11	Eugene
12	Winston
13	Medford
14	Grants Pass

After the CSZ earthquake event, it is anticipated that the affected regions would be without services and assistance for at least 2 weeks (Oregon.gov). The initial days after the earthquake are extremely critical since the affected population will require immediate basic assistance like first aid kits and food. Moreover, displaced people will still be finding their way to relief shelters in the initial few days after the earthquake strikes. For this reason, the relief distribution model in this study is planned for three time periods after the earthquake occurs, where each time period corresponds to a time window of 48 hours. That is, the planning horizon corresponds to a period of six days in the aftermath of an earthquake. With multi-period planning, this model considers changes in the relief supply and demand quantities at different demand nodes on the initial days of the disaster.

In the immediate aftermath of an earthquake, communities are in dire need of basic commodities like shelter, food, water, first aid (including basic medicines), and medical care for injured people. In this study, we consider the distribution of the following commonly required commodities: food, water, and first aid. The Centers for Disease Control and

Prevention (CDC) recommends a daily water requirement of two liters per day for an average adult (cdc.gov). Hence, we estimate that eight pounds of water by weight for a 48-hour time period is the demand per person for this commodity. Similarly, an average person in the US consumes three pounds of food per day (precisionnutrition.com). Therefore, the daily food requirement, which can include instant noodles and bread for three meals per day, is assumed to be six pounds per person in each time period. Since medicine and first aid are lightweight commodities, the first aid commodity is assumed to be one pound per person in each time period for illustration purposes.

5.2.1 Demand Estimation

Demand for each demand node is based on the number of displaced people and number of people needing short-term shelter provided by the Hazus-MH software. We do not include the number of casualties provided by the software, since the casualties include injured people requiring medical attention at a different location and deadly victims of the earthquake event.

Table 5.1 summarizes the demand estimates (in hundreds of pounds) for all the demand nodes for every relief commodity in each time period for Scenario 1 and Scenario 2 for a M9.3 earthquake. The demand estimates for Scenario 3 and Scenario 4 for a M8.0 earthquake are included in Appendix A. The demand is estimated in terms of total weight of food, water or first aid required based on the number of affected people at each demand node. For example, Hazus-MH estimates that 32,540 people will be the population in need in Beaverton, OR. Based on this, demand for food is estimated to be 195,000 pounds, demand for water is 260,000 pounds, and demand for first aid care is 32,500 pounds. The estimated demand for time period 1 is considered to be the baseline demand. Demand estimates for periods 2 and 3 are generated applying a random variation between -15% and 15 % from the baseline demand values.

Table 5.3 *Demand Estimates for M9.3 CSZ Earthquake (in hundreds of pounds)*

Demand Nodes	Relief Commodity	Period 1	Period 2	Period 3
Beaverton	Food	1950	2152	1747
	Water	2600	2883	2821
	Medicine	325	279	338
Portland	Food	3380	3332	3751
	Water	4510	3884	5003
	Medicine	564	529	580
Astoria	Food	25238	274	270
	Water	336	340	319
	Medicine	42	47	40
St Helens	Food	100	104	113
	Water	130	135	133
	Medicine	16	17	16
McMinnville	Food	380	352	346
	Water	506	521	506
	Medicine	63	67	69
Salem	Food	980	962	999
	Water	1310	1242	1206
	Medicine	164	184	158
Dallas	Food	300	324	293
	Water	400	374	395
	Medicine	50	46	47
Newport	Food	250	235	255
	Water	330	362	319
	Medicine	42	38	36
Albany	Food	300	333	308
	Water	401	399	435
	Medicine	50	49	49
Corvallis	Food	720	403	535
	Water	960	634	579
	Medicine	120	75	88
Eugene	Food	1310	1124	1422
	Water	1756	1754	1823
	Medicine	220	194	229
Winston	Food	620	541	611
	Water	820	899	911
	Medicine	100	90	104
Medford	Food	450	416	505
	Water	602	633	614
	Medicine	75	81	86
Grants Pass	Food	238	266	243
	Water	317	308	302
	Medicine	40	45	41

5.2.2 Travel Time Estimation

Earthquakes of high magnitude (i.e., M6.0 and above) can potentially cause severe damage to infrastructures, bridges and roads (Kiremidjian et al., 2007). Due to the destruction that comes with an earthquake, transportation systems are expected to be at a high risk of damage, which in turn can potentially disrupt the travel times and can cause delays. One of the CSZ earthquake scenarios in this study is assumed to be of magnitude M9.3 which would cause severe damage to the ground transportation infrastructure. The travel time delays in the aftermath of an earthquake may become larger due to damaged roads and bridges or closures and blockages from building debris or landslides. The travel delays and damaged state of the roads are accounted for every DC and demand node pair based on the earthquake intensity and its location. After an earthquake strikes, the *a priori* estimated travel time can be considered as a base value and after an initial assessment of the post-disaster conditions of the potential scenarios, the base values can be inflated based on the degree of anticipated damage (Noyan and Kahvecioglu, 2018). The pre-disaster travel times are assumed to be *a priori* ground travel times between every DC and demand node connections and are calculated using Google Maps. The locations of most of the demand nodes in our relief distribution network lie in the range of 4 to 7 for the scaling factor based on the Hazus-MH scale provided in Figure 4.2, with anticipated heavy to violent ground shaking intensity. Based on this assessment, the travel times in the first time period are estimated to be as high as four times the actual travel time. In subsequent days after the disaster occurs, restoration teams start to repair and enable portions of the road transportation infrastructures which gradually reduces the difficulty in transportation between different locations (Wang and Sun, 2023). In this study, time period 3 would be only 5 to 6 days after the earthquake strikes and all road connections would still be in a damaged state. Another important consideration during estimation of the travel time was that the time taken to traverse between any DC and demand node pair should be within the

duration of a single time period, which is 48 hours in our problem. To account for the above mentioned points, transportation time in time period 2 is estimated to be three times the regular travel times, and the transportation times for time period 3 is estimated to be twice the regular travel times.

On the other hand, to estimate the air transportation time, we considered the Euclidean distance between each DC and demand node pair. For example, the distance between the DC in Bend, OR and a demand node in Portland, OR for air transportation is calculated as shown in Figure 5.5. This is done by using one of the many Euclidean distance calculator tools that are available online (www.freemaptools.com). The red line indicates the Euclidean distance used by helicopters providing relief between these two locations. The blue line is the ground transportation route which is used by trucks. To calculate the speed for air transportation, the average speed of a rescue helicopter is assumed to be 110 miles/hr. (Svenson et al., 2006). Air transportation is not affected as much as ground transportation during an earthquake event except for ground infrastructure required for takeoff and landing activities. Since helicopters do not require any elaborate ground infrastructure, travel time delays in air transportation (for helicopters) are not considered. Furthermore, since the road blockages and road closures do not affect the air transportation travel times, the travel times for this mode of transportation are considered to be same for all three time periods.

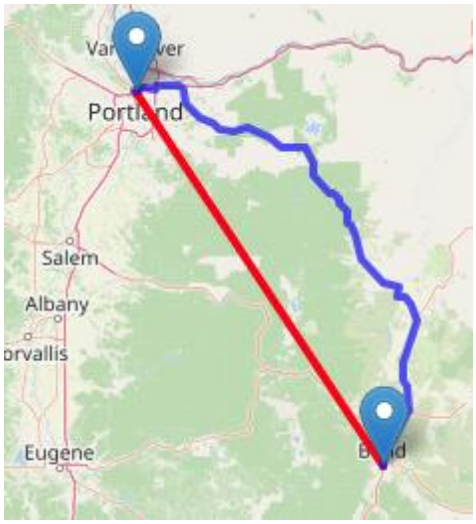

Figure 5.5 *Example of Euclidean Distance for Air Travel Time Estimation*

5.2.3 Cost Estimation

Transportation costs are calculated based on the time required for a one-way trip between each DC and demand node. To estimate ground transportation travel time and air transportation travel time, we adopted the method proposed by Barbarosoğlu and Arda (2004). In this approach, all transportation costs are assumed to be a linear function of the time taken to travel the distance between each DC and demand node pair. As discussed in the previous section, actual distances are used for ground transportation and Euclidean distances are used for air transportation. Since the time estimate for all the connections already considers the delays due to road blockages and damage, the transportation cost incorporates the increased cost in each period as well. The cost associated with ground transportation per unit distance travelled, is assumed to be cheaper than the cost associated with air transportation with the cost for air transportation being twice the cost for ground transportation as proposed by Barbarosoğlu and Arda (2004). The per unit transportation cost for ground transportation is assumed to be $1 per minute.

5.2.4 Supply Estimation

At the time of a disaster, basic relief commodities for the affected people are collected from various sources including government agencies, non-governmental organizations (NGOs), international aid organizations, and donations from individuals and businesses (USDA Foods Disaster Manual, 2021). Government agencies in the United States, such as FEMA, have provisions for providing food and other essential supplies to the disaster hit regions though various disaster response programs. Because of the uncertainty associated with the supply, it is not possible to accurately estimate the availability of supply commodities for food, water and first aid. For this study, an estimate of the supply available at each DC is derived as a percentage of the total demand for each commodity in time period 1 divided by the number of available DCs. In the moments immediately after a large-scale earthquake disaster, the supply quantities are always insufficient (Huang and Refeii, 2019; Wang and Sun, 2023). For this reason, the available supply is assumed to be 80% of the demand in time period 1. To create variation in the available supply at each DC, individual values are randomly varied between ± 5% for the time period 1 quantity at each DC. As the disaster hit region receives aid from various organizations to satisfy the demand of the population in need, the available supply in time period 2 and time period 3 are varied randomly between 5% to 20% of the available supply for time period 1 for each commodity to account for supply fluctuations.

5.2.5 Other Input Parameter Data

- It is assumed that temporary buildings will be used which will act as DCs in this relief network. The average monthly rate for a storage unit in the Portland, OR region is around $100 for 10x10 square feet of storage space (storagearea.com). We assume the approximate size of the DC to be 25,000 square feet, which is the average area of a large retail store (vts.com). This area is assumed enough to store large quantities of relief commodities for a large number of people. Based on this area, the fixed cost

associated with the establishment of any of the DCs is randomly generated between [$20,000, $30,000] for the length of the planning horizon.

- The total budget to establish the DCs and carry out the relief distribution in a post-disaster scenario after an earthquake is set to be $12 million that is based on the average budget granted by FEMA for rescue operations of various disaster for different US states (fema.gov).

6. Computational Experimentation Results

The performance of the proposed model presented in Chapter 4 was tested using scenarios for the case study described in Chapter 5. Since the problem has two objectives, the model was solved using the lexicographic method to evaluate the trade-off between the minimization of the total travel time and total unmet demand across the three time periods in the planning horizon. This section contains the description of the case study setup, the numerical results for the computational experimentation performed, and a discussion of the implications of these results.

6.1 Case Study Setup

The performance of the proposed model is tested using the case study for a CSZ earthquake event in the state of Oregon presented in Chapter 5. Four scenarios were developed as presented above in Figure 5.3. For all four scenarios, the value of the minimum percentage of demand to be fulfilled (Δ) was set to 65%. The allowed deviation from the average demand (δ) for each commodity in each period was set to 10%. A total of 50 large trucks each with a capacity of 20 tons (40,000 pounds), and a set of 30 helicopters each with a load capacity of 4,000 pounds are available for each scenario. It is assumed that the same set of trucks and helicopters will be used across all three periods in every scenario. The number of people affected by the disaster was estimated from Hazus-MH and all other input parameters were generated as discussed in Chapter 5. Since the DC located in Junction City, OR is the closest to the epicenter of the CSZ earthquake modeled for the case study, this DC location is not available for Scenarios 2 and 4 with one unavailable DC. A summary of the parameters used for the four earthquake scenarios in our study are summarized in Table 6.1 and the results are presented in the following section.

Table 6.1 *Parameters for CSZ Earthquake Scenarios*

Scenario	Earthquake Magnitude	Candidate DCs	Demand Threshold (Δ)	Allowable Demand Deviation (δ)	Trucks	Helicopters
1	M9.3	All available	65%	±10%	50	30
2	M9.3	1 unavailable	65%	±10%	50	30
3	M8.0	All available	65%	±10%	50	30
4	M8.0	1 unavailable	65%	±10%	50	30

6.2 Numerical Results for CSZ Earthquake Scenarios

A multi-objective optimization problem involves finding a set of solutions that optimize multiple objectives simultaneously, which often conflict with each other. In contrast to a single-objective optimization problem, which seeks to find a single optimal solution, a multi-objective optimization problem seeks to find a set of optimal solutions, also known as Pareto optimal solutions that simultaneously optimize all the objectives. A solution is said to be efficient, non-dominated or Pareto optimal in an objective space, if none of the objectives can be improved without sacrificing or deteriorating other objective values (Wang and Rangaiah, 2017). A Pareto optimal solution is, therefore, a feasible solution that is not dominated by any other solution and an improvement in any one objective is only possible at the expense of a worse solution in at least one other objective (Ravindran, 2007). The set of all these non-dominated solutions, called the Pareto frontier, is commonly used to evaluate trade-offs between conflicting objectives and provides the set of solutions that gives the best compromise between the multiple objectives. Although the Pareto optimal solutions are non-dominated, all solutions are not equally desired. The Pareto frontier scatter plot is widely used for visually evaluating the trade-offs between the objectives in a multi-criteria solution space. Analyzing the Pareto fronts helps in making informed decisions about which solution to choose based on the specific needs and preferences of the decision makers for the problem at hand.

A Pareto frontier approximation is created for the proposed bi-objective optimization model in this research. To find the set of Pareto optimal solutions and to create a Pareto front, the value of Objective 1 (unmet demand) is allowed to degrade relative to Objective 2 (total travel time) by small successive increments until the value of Objective 2 approximates to zero. The relative tolerance is varied in discrete steps between 0% to 30% in increments of 1%. The lexicographic method was applied iteratively with the relative tolerances, and the corresponding optimal solutions were stored and plotted. The resulting graph provides a Pareto frontier for the multi-objective optimization problem.

Figure 6.2 shows the Pareto frontiers for Scenarios 1 and 3 when all DCs are available to satisfy post-disaster relief demand. Similarly, Figure 6.3 shows the Pareto frontiers for Scenarios 2 and 4 when one candidate DC is unavailable to satisfy post-disaster relief demand. Since Scenario 2 and Scenario 4 have only 5 available candidate DCs, the Pareto frontiers for these scenarios were in a different range of values for the two objectives than the Pareto frontiers for Scenario 1 and Scenario 2. Therefore, two separate Pareto frontiers were created to accommodate the differences in the range of total unmet demand and total travel time.

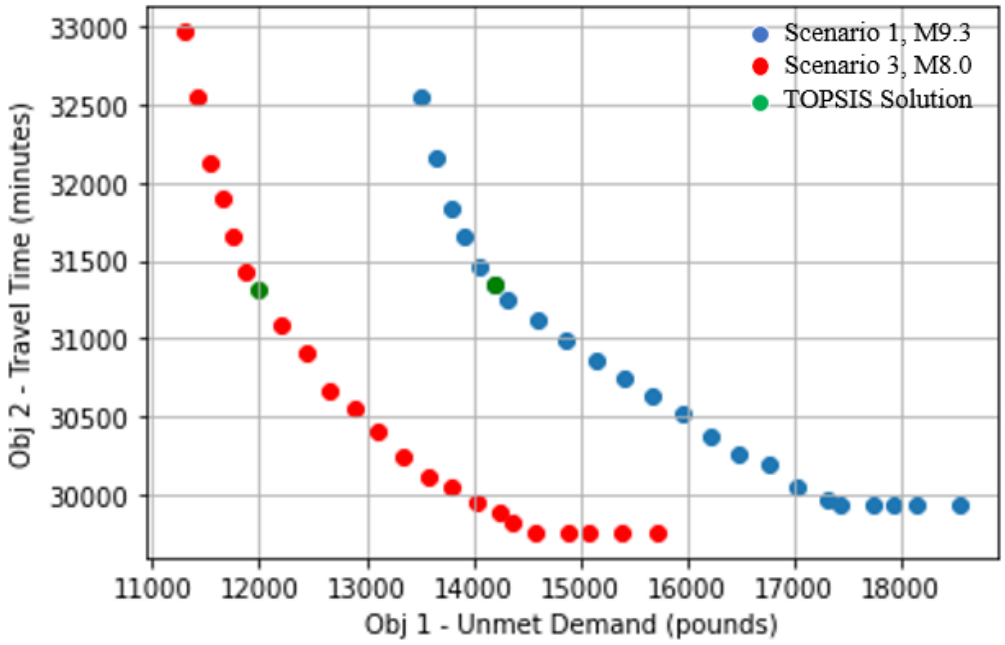

Figure 6.1 *Pareto Optimal Solutions for Earthquake Magnitudes M9.3 and M8.0 with Six Candidate DCs Available (Scenario 1 and Scenario 3)*

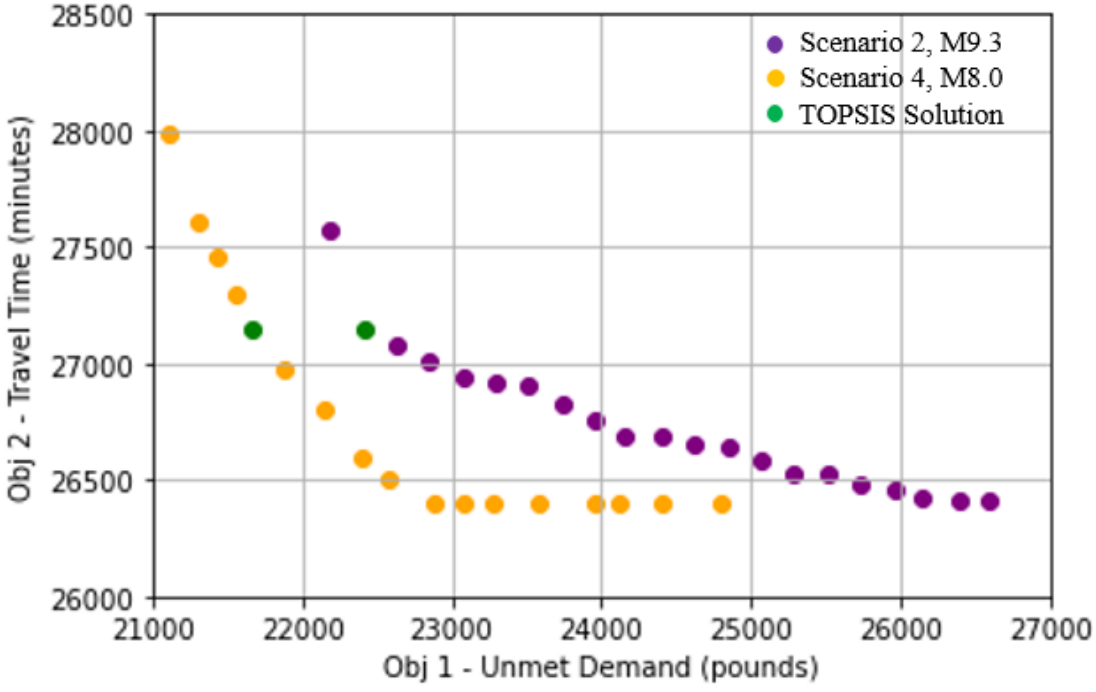

Figure 6.2 *Pareto Optimal Solutions for Earthquake Magnitudes M9.3 and M8.0 with Only Five Candidate DCs Available (Scenario 2 and Scenario 4)*

Since all solutions in a Pareto frontier are optimal, policy makers may choose any solution that represents a balance between the conflicting objectives according to the situation at hand. For our research, we use a multi-criteria decision-making technique called Technique for Order of Preference by Similarity to an Ideal Solution (TOPSIS) method developed by Hwang and Yoon (1981) to help us identify a compromise solution from our Pareto frontier. The TOPSIS method suggests a compromise ranking by identifying solutions with shortest distance from the positive-ideal solution and furthest distance from the negative-ideal solution in a given set of non-dominated solutions. The TOPSIS solution may not necessarily represent the best solution from the Pareto set and is determined for illustration purposes only. The TOPSIS solutions in the Pareto frontiers in Figure 6.2 and Figure 6.3 are identified by green points.

Table 6.2 summarizes the TOPSIS results for all four CSZ earthquake scenarios. Decision variable values for the TOPSIS solution for Scenario 1 are provided in Appendix B. For Scenario 1 (M9.3) and Scenario 3 (M8.0) when all the candidate DCs are available, unmet demand is the lowest. However in Scenario 1 and Scenario 3, since more supply is distributed to the demand nodes in each period, the total air and ground transportation travel times are higher than those for Scenario 2 and Scenario 4, respectively. It is observed that for Scenario 2 and Scenario 4, the unmet demand is significantly higher than for the other two scenarios. This is due to the unavailability of one of the candidate DCs which significantly reduces the total supply of relief commodities in all periods. As the total available supply in these scenarios is lower than the demand, all the six DCs remain open in all three periods to minimize the unmet demand. Moreover, due to the supply shortages, the model forces all the available supply to be distributed across all three time periods. From Table 6.2, it is also observed that Scenario 1 required the highest number of trucks and helicopters. According to the results from the application of the model across the four scenarios, a maximum of 48 trucks and 26 helicopters

would be required for the post-disaster relief distribution for a three-period problem covering six days after the onset of a CSZ earthquake.

Table 6.2 *Numerical Results for TOPSIS Solutions for All Four Scenarios*

Scen.	Mag.	Avail. DCs (#)	Demand Th. (Δ)	Allowed Dev. (δ)	Obj1 (lb)	Obj2 (min)	Trucks (#)	Heli. (#)	Total Cost ($)	CPU (sec)	Cost Var. (%)
1	M9.3	6	65%	10%	14,191	31,340	48	26	10,917,847	482	-
2	M9.3	5	65%	10%	22,406	27,145	43	22	10,706,514	355	-1.90
3	M8.0	6	65%	10%	11,986	30,310	36	20	8,645,797	648	-20.80
4	M8.0	5	65%	10%	21,312	25,458	32	19	8,474,815	701	-22.30

Table 6.2 also summarizes the variation in total cost for each scenario with respect to Scenario 1 that is considered as the base scenario. The reduction in total cost for Scenarios 2, 3, and 4 is due in part to the reduced number of trucks and helicopters used in these scenarios. Also, the reduction of supply available for transport due to the unavailability of one of the DCs in Scenario 2 and Scenario 4 contributes to the reduction in total cost with respect to Scenario 1. The computational (CPU) time to run the model for the four scenarios is also specified in Table 6.2.

In the next section, we investigate the effects of different values for some of the problem parameters for the baseline case in Scenario 1 to explore their influence on the total unmet demand, the total travel time and the relief distribution pattern for all demand nodes across each time period.

6.3. Sensitivity Analysis of Baseline Case (Scenario 1)

Analyzing the effect of varying different parameter values in the model helps us to understand the tradeoffs between different values for these parameters and the outcomes of the model. The insights from these outcomes and the observed tradeoffs can help decision makers as they consider the different objectives for post-disaster relief distribution planning. In this section,

we investigate the effects on the Scenario 1 TOPSIS solution of varying the values of allowable deviation percentage from demand average (δ), demand threshold (Δ), budget, and number of vehicles available for relief distribution.

6.3.1 Effect of Varying δ

We first investigate the effect of varying the allowable deviation percentage from the average met demand (δ) on the relief distribution pattern across different demand nodes and the total travel time for the Scenario 1 TOPSIS solution. To understand the efficacy of an equitable distribution obtained by applying the permissible deviation from average demand constraint, we compare the numerical results obtained by varying the values of δ from the baseline value of 10% to 5% (i.e., more equitable distribution) and to 100% (i.e., no equitable distribution considered). This would provide insight into how the relief distribution pattern would change as we tighten the value of δ in case of relief commodity shortages. The results are presented in Table 6.3.

Table 6.3 *Scenario 1 TOPSIS Results with Different Values of δ*

Earthquake Magnitude	M9.3	M9.3	M9.3
Min demand % at each node	65%	65%	65%
Deviation allowed (δ)	**10%**	**5%**	**100%**
Computational Time (sec)	852	2,444	258
Unmet Demand (pounds)	14,191	14,191	14,191
Travel Time (min)	31,340	31,675	30,905
Trucks (#)	48	48	47
Helicopters (#)	26	28	25
Total Cost ($)	10,571,847	10,877,624	10,278,643
Cost Variation	-	2.90%	-2.77%

Table 6.3 shows that the total unmet demand for all three cases remains the same (since supply is limited), but the overall travel time across all three periods is higher with δ = 5%. Furthermore, since the model becomes more restricted as we reduce the value of δ, the

computational time for δ = 5% is the highest. Table 6.3 also summarizes the total cost for the entire relief distribution operation across all three time periods for different values of δ. When the total cost for δ = 10% is considered as the base value, the total cost increases by 2.9% for δ = 5%. This is because the model is forced to distribute the relief supplies more equitably across all the demand nodes for all three periods. The increase in cost is also due to the increase in the number of vehicles used for δ = 5% (with two more helicopters). On the other hand, the total cost is 2.77% lower than the base case value for δ = 100% since the model is relaxed with respect to equitable distribution and the number of vehicles used is also reduced.

Figures 6.3, 6.4 and 6.5 show the comparison of relief distribution to all demand nodes for all commodities for the different values of δ across all three periods, respectively. The average demand for every commodity in a period is denoted by the red line, while the black dotted line represents the upper and lower limits for demand satisfaction. After comparing the results obtained from the model in Figures 6.3, 6.4 and 6.5 it is evident that the relief distribution for δ = 5% is the most equitable for all commodities across every period. It can be observed that the relief distribution for δ = 100% is not equitable, as some of the demand nodes receive 100% of the relief supplies, while other demand nodes receive only the minimum demand threshold.

As the total unmet demand remains the same for all cases, the above findings suggest that in case of relief commodity shortages, enforcing the constraint limiting the deviation from the average demand allows for the relief distribution to be equitable and prevents an unfair allocation of relief supplies, such that no particular demand node is at a higher disadvantage. There is a clear tradeoff between equitable distribution and the total travel time. As the relief distribution becomes more equitable, the travel time increases. Based on the amount of relief supplies available, the model helps the decision makers to make better choices in order to make the relief distribution plan fair and equitable.

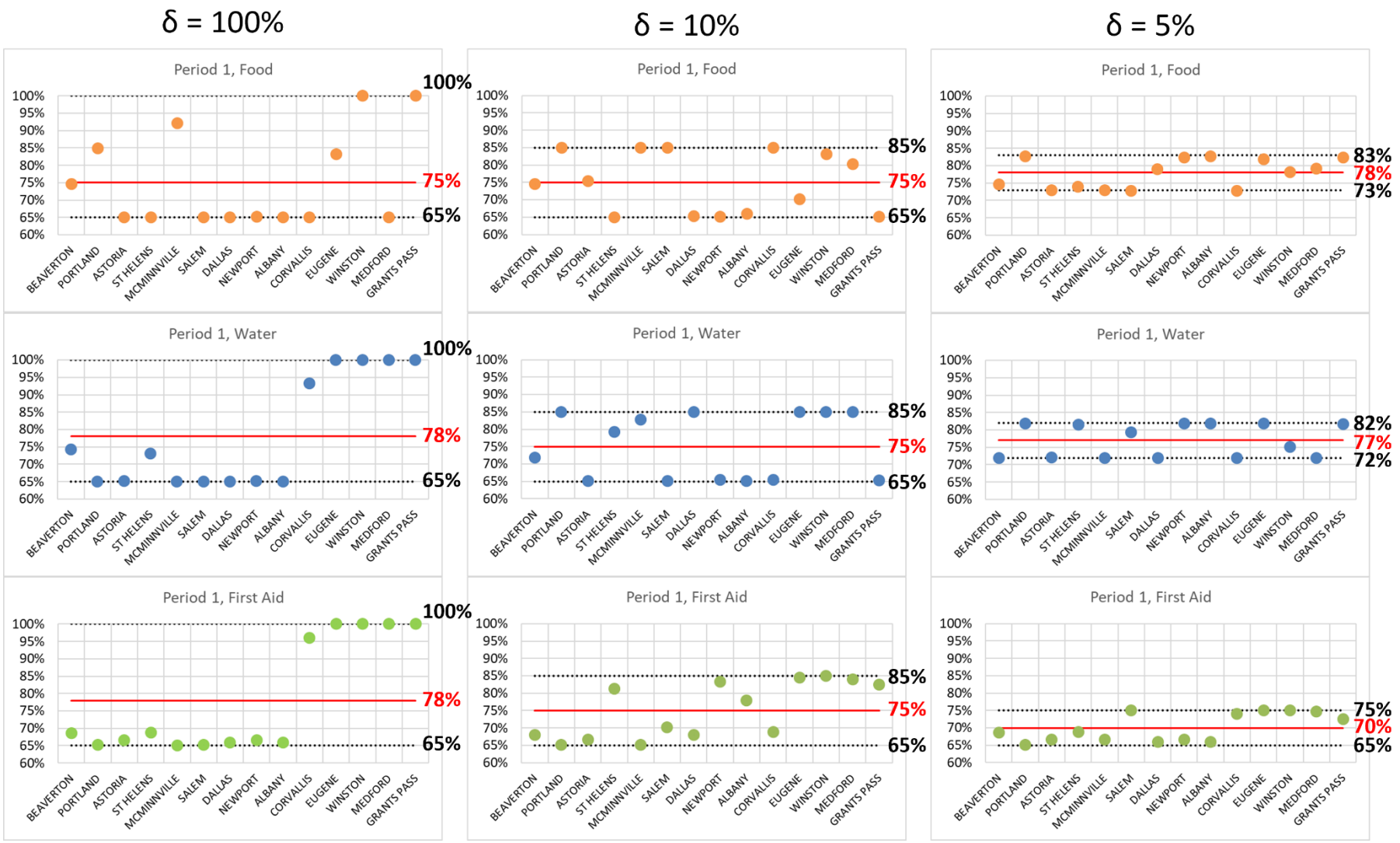

Figure 6.3 *Comparison of Relief Distribution for All Commodities in Period 1 for Different Values of δ*

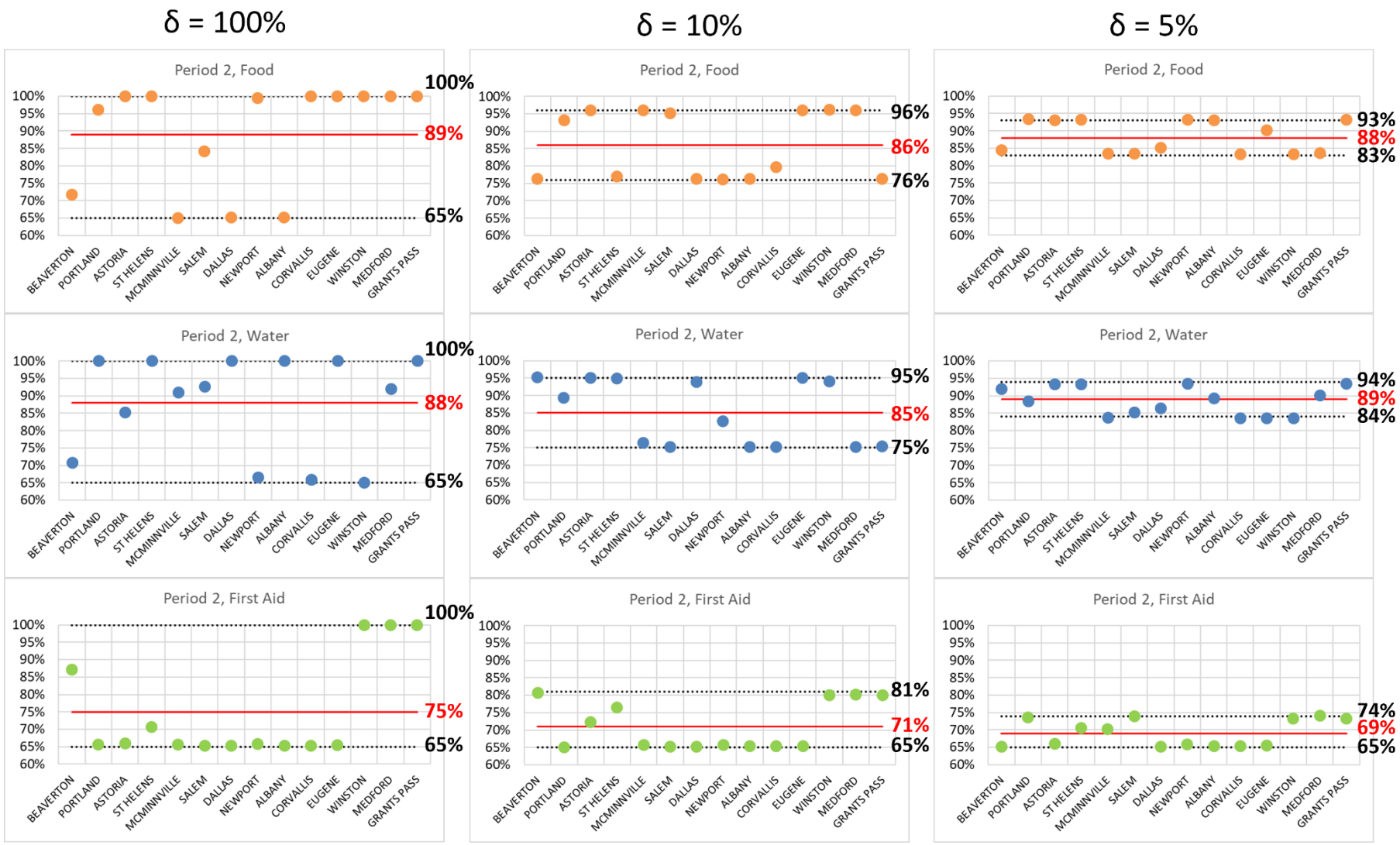

Figure 6.4 *Comparison of Relief Distribution for All Commodities in Period 2 for Different Values of δ*

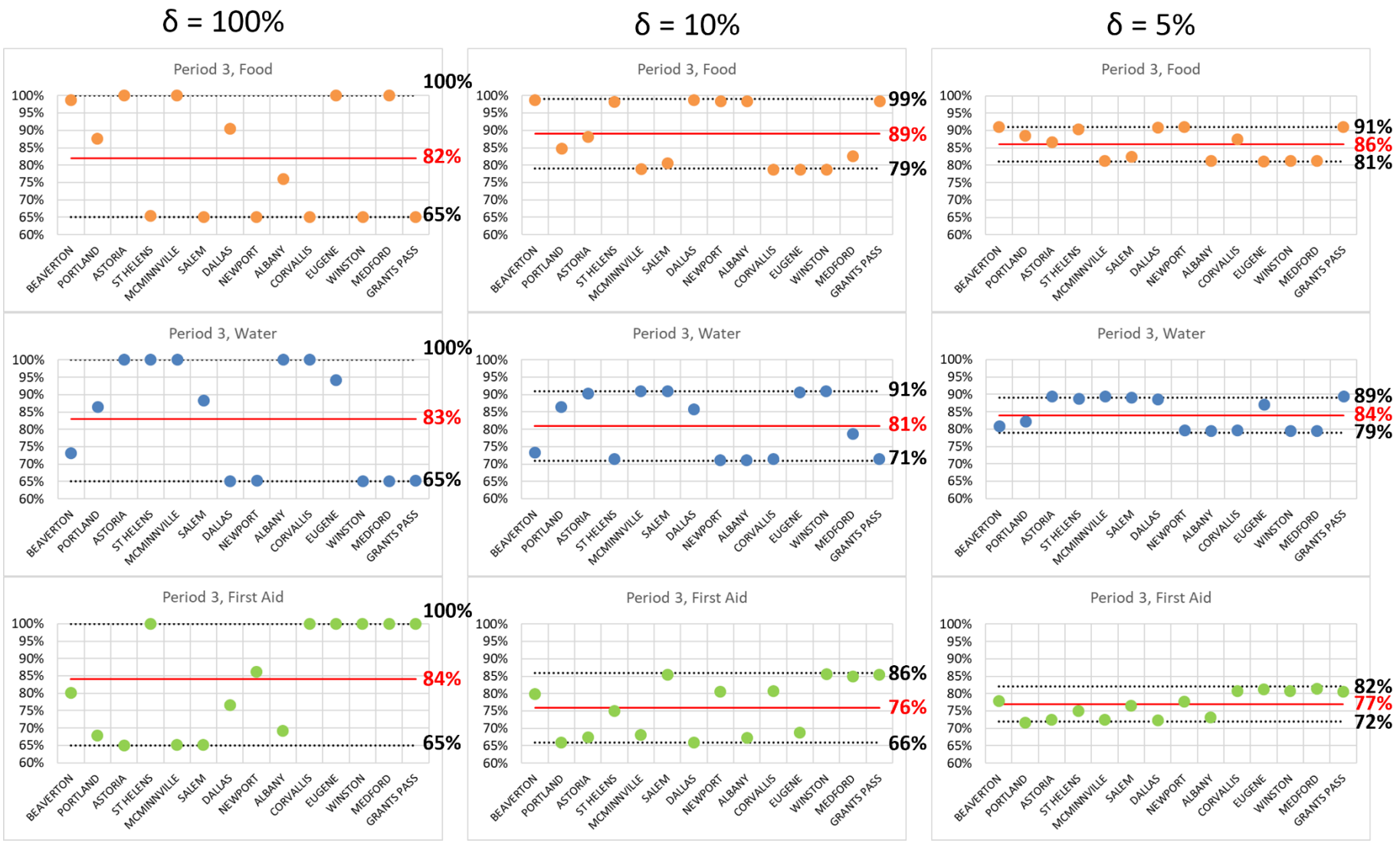

Figure 6.5 *Comparison of Relief Distribution for All Commodities in Period 3 for Different Values of δ*

6.3.2 Effect of Varying Minimum Demand Threshold Δ

We also investigate the effect of varying the value of the minimum demand threshold for the Scenario 1 TOPSIS solution when keeping the allowed deviation from the average demand value δ = 10%. Since the first objective is to minimize the unmet demand, the model will strive to reduce the unmet demand by always prioritizing to distribute the entire available supply for every commodity across all three periods. Varying the demand threshold will only set a lower bound on the minimum percentage of demand satisfaction for every commodity in all periods while the supply exists to meet the threshold. This does not prevent the model from maximizing the distribution of the relief commodities within the available vehicle capacity and the available budget. Table 6.4 summarizes the results from varying the minimum demand threshold Δ values between 55% and 85% for the Scenario 1 TOPSIS solution.

Table 6.4 *Results of Varying the Minimum Demand Threshold Value Δ*

Demand Threshold (Δ)	Obj 1 Value (pounds)	Obj 2 Value (min)	Trucks (#)	Helicopters (#)	Total Cost ($)	Computational Time (sec)
55%	14,191	31,000	47	25	10,783,936	415
60%	14,191	31,110	47	26	10,867,341	691
65%	14,191	31,340	48	26	10,917,847	852
70%	14,191	31,705	47	27	10,940,204	908
75%	14,191	32,635	48	26	10,924,946	1,068
77%	14,191	33,130	48	27	10,939,775	2,207
80%	*infeasible*	-	-	-	-	-
85%	*infeasible*	-	-	-	-	-

As observed in Table 6.4, varying the minimum demand threshold value does not affect the total unmet demand (Obj 1) as all of the supply is still distributed with the available vehicles and budget. As discussed earlier, the minimum demand threshold value only enforces the

minimum demand satisfaction percentage any demand node should receive, but does not prevent the model from maximizing the allocation of relief supplies either by trucks or helicopters. Increasing the minimum demand threshold percentage causes a modest increase in the number of trucks and helicopters used as well as the total cost. These variations are due to the changes in the allocation of relief supplies within the three time periods and the corresponding transportation costs for the distribution of relief commodities across the three time periods. Furthermore, in the baseline case with relief supply shortages, the model can enforce a minimum demand threshold as high as 77% and still feasibly distribute relief commodities equitably. For the instance with the highest possible minimum demand threshold value, the total travel time (Obj 2) represents a 6.4% increase with respect to total time for the instance with a minimum demand threshold of 55%. On the other hand, the increase in total cost between the two extreme instances is 1.5%. Finally, the computational time increases as the minimum demand threshold value increases. The computational time for the instance with the highest minimum demand threshold is five times higher than the instance with minimum demand threshold of 55%.

6.3.3 Effect of Surplus Supply

All previous instances correspond to situations in which supply shortages exist. In these scenarios, the model selects all the candidate DCs to remain open in order to distribute all of the available supply and minimize the total unmet demand. To evaluate situations in which the selection of which candidate DC should be open and which should remain closed, the supply is assumed to be in surplus. We investigate the effects of surplus supply for total available budget values of $8 million and $5 million. The parameter values used for these cases are summarized in Table 6.5.

Table 6.5 *Parameter Values for Surplus Supply Cases*

Earthquake Magnitude	M9.3
Min demand % at each node	65%
Deviation allowed	10%
Available Trucks (#)	50
Available Helicopters (#)	30

Table 6.6 summarizes the status of all DCs across all three periods for both budget values. The check mark (✓) represents open DCs and the cross (✕) represents closed DCs for the specified time period. For a budget of $8 million, as the supply is able to fulfill the demand, total unmet demand is observed to be zero. Moreover, the total travel time is 22,160 minutes and the total cost is $7.61 million, which is 30.23% lower than the cost when all the DCs are open. When the budget is further reduced to $5 million, more DCs remain closed in certain periods and the unmet demand across all periods increases. Along with the closure of the DC located at Madras, OR for all three periods, the DC located at Bend, OR remains closed for period 2 and period 3. The total travel time is reduced to 18,740 minutes, but the unmet demand increases to 10,184 pounds. The results for both budget values are summarized in Table 6.7. The total cost consists of costs associated with opening DCs and the transportation costs associated with using a truck or helicopter between every DC and demand node pair. The reduction in the overall cost associated with only five DCs is because fewer relief commodities are supplied in the network.

Table 6.6 *Status of Distribution Centers for Scenario 1 with Surplus Supply*

Period	DC	Status ($8 Million)	Status ($5 Million)
1	SANDY	✓	✓
1	OREGON CITY	✓	✓
1	ROSEBURG	✓	✓
1	MADRAS	×	×
1	BEND	✓	✓
1	JUNCTION CITY	✓	✓
2	SANDY	✓	✓
2	OREGON CITY	✓	✓
2	ROSEBURG	✓	✓
2	MADRAS	×	×
2	BEND	✓	×
2	JUNCTION CITY	✓	✓
3	SANDY	✓	✓
3	OREGON CITY	✓	✓
3	ROSEBURG	✓	✓
3	MADRAS	×	×
3	BEND	✓	×
3	JUNCTION CITY	✓	✓

Table 6.7 *Results Summary for Scenario1 with Surplus Supply*

Total Available Budget	$8 Million	$5 Million
Computational Time (sec)	450	1,023
Objective 1 (Unmet Demand - pounds)	0	10,184
Objective 2 (Travel Time - min)	22,160	18,740
Total Cost ($)	7,616,872	5,000,000
Trucks (#)	49	48
Helicopters (#)	30	28

6.3.4 Effect of Available Trucks and Helicopters

Up to this point, the model has been tested with a total of 50 available trucks and 30 helicopters. In this section, we investigate the effect of varying the number of trucks and helicopters on the total unmet demand and travel time for the Scenario 1 TOPSIS solution. We reduce the number of total available trucks to 45 and the total available helicopters to 15. By reducing the number of available vehicles, we investigate the effects of vehicle shortages in the relief distribution

pattern in the network. Table 6.8 shows the parameter values used to investigate the effects of vehicle shortages in the total unmet demand and total travel time. The results are summarized in Table 6.9 and are compared to the result for the baseline scenario with no vehicle shortages.

Table 6.8 *Parameter Values for Scenario 1 with Vehicle Shortages*

Earthquake Magnitude	M9.3
Min Demand % at Each Node	65%
Deviation Allowed	10%
Total Budget ($)	12 Million
Available Trucks (#)	45
Available Helicopters (#)	15

Table 6.9 *Results Summary for Scenario 1 with and without Vehicle Shortages*

	Vehicle Shortages	No Vehicle Shortages
Computational Time (sec)	1,178	482
Objective 1 (Unmet Demand – pounds)	18,368	14,191
Objective 2 (Travel Time – min)	26,160	31,340
Total Cost ($)	9,245,387	10,917,847
Trucks (#)	45	48
Helicopters (#)	15	26

With fewer available vehicles, the total unmet demand increases 30% when compared to the baseline scenario as fewer relief commodities are distributed from the DCs to demand nodes. Therefore, the total travel time also reduces as compared to the baseline scenario.

To get more insight into how much impact adding a single truck or helicopter has on the objective functions and the total cost of the relief operation, we ran the model by incrementing the total number of available trucks in increments of one from 45 until 50, while keeping the total number of available helicopters at 15. We then incremented the total number of available helicopters in increments of one from 15 to 20 while keeping the total number of available trucks at 45. The results for these instances are depicted in Figure 6.6 and Figure 6.7, respectively. From Figure 6.6 and Figure 6.7 it can be seen that adding more trucks allows to

distribute more relief commodities across the different demand nodes than adding helicopters. Although a helicopter can reduce the total travel time, it has a marginal impact on the demand satisfaction rate as they have lower loading capacity. This representation of the relative variations can help policy makers to understand the trade-off between the total unmet demand and total travel time so that informed decisions can be made for the problem at hand.

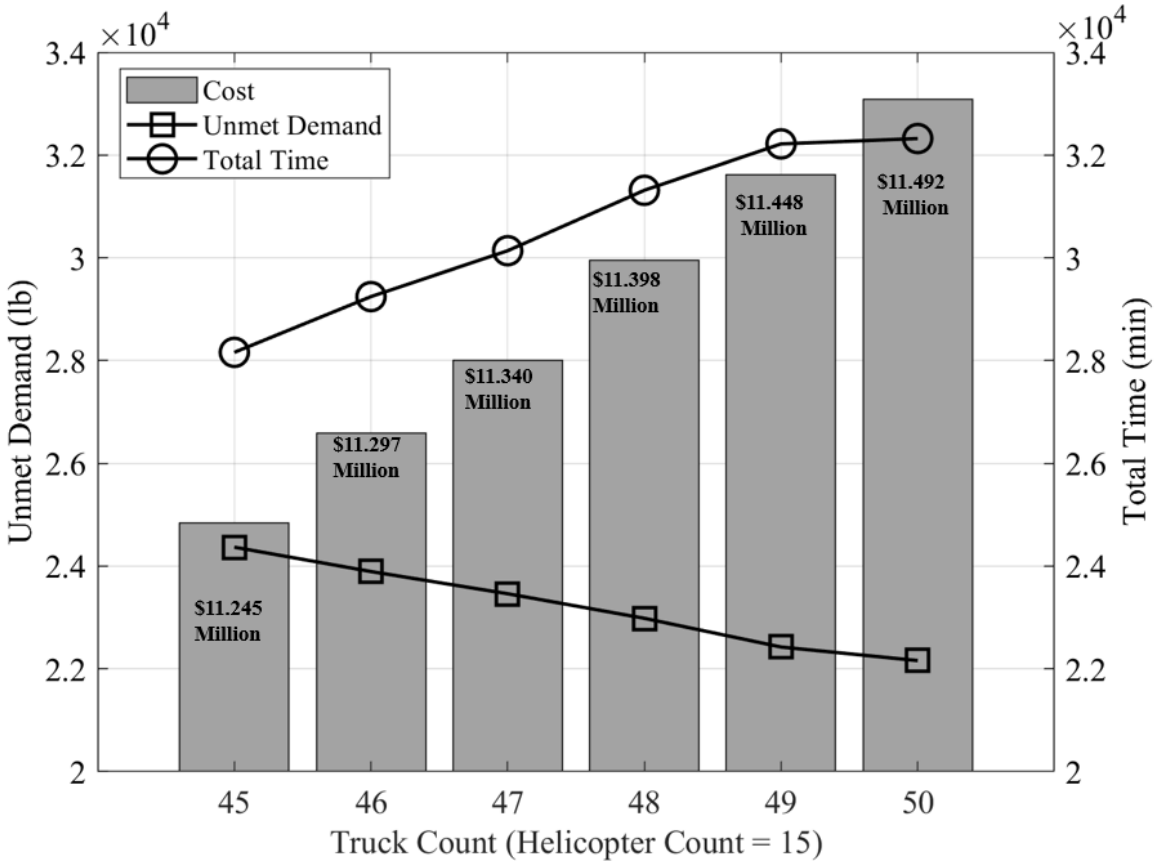

Figure 6.6 *Effect of Varying Number of Trucks on the Objective Functions and Total Cost for Scenario 1*

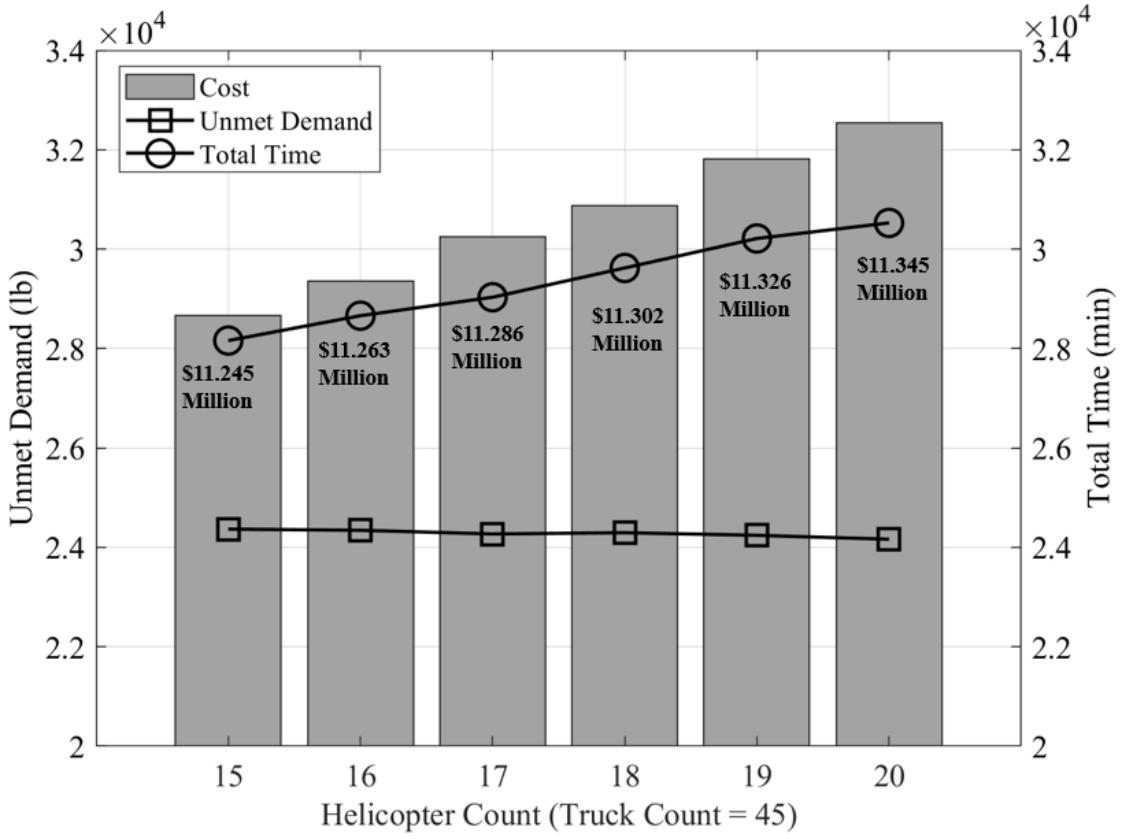

Figure 6.7 *Effect of Varying Number of Helicopters on the Objective Functions and Total Cost for Scenario 1*

6.4 Discussion

The results in the previous sub-sections present some insightful and interesting findings from the evaluation of the effects of varying the permissible deviation percentage from the average demand (δ), the minimum demand threshold (Δ), supply values, and the number of trucks and helicopters available. In this section we present a summary of the most significant observations and discuss their implications.

First, we demonstrate the model's effectiveness for equitable distribution of relief commodities, when supplies are insufficient to satisfy all of the demand. It can be inferred that,

in case of relief shortages, the model enforces the relief distribution in an equitable manner, such that no particular demand node is at a higher disadvantage while keeping the total unmet demand the same for all values of δ. As the model is made tighter by varying the permissible deviation from 10% to 5%, the total cost increases by almost 3% with a slight increase in the travel time. Although the increase in cost is relatively small, having a δ of 5% significantly improves the relief distribution pattern from an equity perspective as compared to results with δ of 100%. The model is able to achieve equitable distribution with relatively small increases in the total cost and total travel time; however, the computational time to run the model is three times as high.

Increasing the minimum demand threshold (Δ) increases the total travel time and the total cost of the operation, given additional relief commodities that are distributed across all the demand nodes. Moreover, it only causes a modest increase in the number of trucks and helicopters used. However, it has no impact on the total unmet demand for all three periods. The demand threshold only enforces the minimum demand satisfaction percentage any demand node can receive either by truck or by helicopter but does not prevent the model from maximizing the allocation of relief supplies. The total computational time to run the model for the different values of Δ ranged from 415 seconds to 2,204 seconds. Setting the threshold value to the highest feasible value would help in achieving a high level of service for all demand nodes in all three time periods.

Next, we evaluated instances with surplus supply for available budget quantities of $8 million and $5 million. In these instances, the DCs at Madras, OR and Bend, OR are not selected to be operational since they will incur additional cost and time to distribute the relief commodities across all demand nodes. This insight could help the decision-makers to choose the location of available DCs to maximize the overall efficiency in the relief distribution operation.

Finally, we vary the total number of trucks and helicopters available in the relief distribution network to investigate their effect on the total unmet demand and the total travel time. To achieve this, the total number of available trucks is reduced from 50 to 45 and the total number of available helicopters is reduced from 30 to 15. The shortage in vehicles results in a significant impact on the total unmet demand. The increase in the unmet demand is 30% higher than the unmet demand for the baseline scenario.

The model was run for different number of available vehicles to understand the impact of addition of a single truck versus addition of a single helicopter on the unmet demand and the total travel time. Addition of a single truck has a significant impact on reducing the total unmet demand versus the addition of a single helicopter. However, the cost as well as the travel time also increase in order to satisfy the demand of a higher number of demand nodes. On the other hand, the addition of a single helicopter has an insignificant impact in reducing the unmet demand, although the travel time reduces slightly with very less impact on the total cost of the relief distribution operation.

In conclusion, analysis of the various parameters suggests that the number of vehicles involved in the relief distribution operation has the most significant impact on the total unmet demand in the relief distribution operation. Given a choice between adding more trucks or helicopters, the results from the application of the model suggest that adding trucks would be more beneficial to minimize the total unmet demand than the addition of helicopters at the trade-off of a slight increase in the total travel time. While helicopters provide the advantage of being able to access remote and inaccessible areas, their limited carrying capacity makes them less efficient for large-scale relief distribution. If the affected areas have limited roads or are severely damaged, helicopters may still be necessary to reach those locations. Therefore, a balanced approach that combines both trucks and helicopters, based on the specific circumstances and requirements of the relief operation, would be the most effective strategy.

The results from the model also suggest that defining a range of permissible deviation in demand satisfaction with respect to the average demand for all nodes is effective at obtaining an equitable relief distribution pattern for serving all demand nodes in the region. Based on the available supply of relief commodities, decision makers can choose a suitable value for the permissible deviation δ that would allow them to distribute the available supply so that no particular demand node is at disadvantage. Finally, the model also helps in the identification of the most efficient candidate locations for the placement of DCs, which effectively minimizes both the total unmet demand and the total travel time. This can further enhance the effectiveness of the relief distribution operation.

7. Conclusions and Future Work

At the time of a disaster when relief supplies are insufficient, efficient and equitable distribution of multiple relief commodities is required to meet the needs of the affected population within a fixed budget and in a short span of time. Planning a robust and flexible relief distribution network is crucial to reduce the impact of the disaster.

In this research, we developed a multi-objective mixed integer programming model for relief distribution with the primary objective of minimizing the total unmet demand for relief commodities and the secondary objective to minimize the total travel time for an equitable relief distribution to demand nodes. The formulation considers multiple commodities, multiple modes of transportation and multiple periods in a planning horizon after the onset of an earthquake. The relief distribution network consists of multiple candidate distribution center (DC) locations that are selected based on the damage and intensity of the earthquake, and multiple demand nodes that are located in cities with the anticipated highest number of affected people. Equity in the relief distribution is achieved by a combination of minimizing the total unmet demand for all commodities across all time periods, and restricting the deviation in the demand satisfaction rate for each demand node to be within a specified range. Based on the intensity of relief shortages at the time of the disaster, this model will aid the decision makers to define a specific target for demand satisfaction that can be fulfilled in an equitable manner. This will ensure that at the time of relief shortages, no particular community is at a higher risk of disadvantage with respect to others.

We tested the model by conducting a computational experiment using a case study for a CSZ earthquake in the state of Oregon. We generated The model was tested on four different earthquake scenarios with two different earthquake magnitudes and different levels of availability of candidate DCs. The model is solved using a lexicographic approach to provide

Pareto optimal solutions which consider the trade-offs between the total unmet demand and the total travel time under a deterministic disruption scenario. In addition, a sensitivity analysis was performed to understand the effects of uncertainty on the values of the fundamental parameters of the relief distribution model on the solutions obtained for one of the generated scenarios. The model insights and the optimal solutions obtained with the proposed model are applicable to the specific problem instance and the earthquake scenario for which it was evaluated (Scenario 1).

The model proposed in the current research could help decision makers to make strategic decisions regarding the placement of candidate DCs and to make efficient and equitable tactical decisions about the quantities of relief commodities to be distributed between the DCs and the demand nodes using different modes of transportation. Furthermore, this research study provides insights that might be valuable to the decision makers in planning a robust and flexible relief distribution network in anticipation of a disaster. For example, the model suggests that if the demand nodes are accessible by road, addition of more trucks would be more advantageous in minimizing the total unmet demand, than the addition of helicopters with only a slight increase in the total travel time. The understanding of the effects of the different parameters would also help the decision makers to improve the design and operation of the relief distribution network when limited resources are available like choosing the most efficient DC locations and finding the highest achievable demand threshold that can be satisfied equitably for all demand nodes.

We acknowledge that the conclusions from this research are based on the particular instances that have been evaluated in this study and not generalizable for other instances with different scale and disaster types. More work is required to improve the proposed model and to develop additional insights that could be generalizable. One of the limitations of this research is that in the case of surplus supply, the model does not calculate the quantity of unused relief

commodities at the end of each period so that they can be made available in future periods. One way to address this would be to add constraints to keep track of the inventory level for each commodity at each DC at the end of each time period, which can then be carried over to the next time period in addition to the incoming supply of relief commodities available in that period .

Another limitation is that the model only considers equity in terms of quantity of relief commodities received by the different demand nodes. To further expand the capabilities of the model, equity can be extended to other relevant aspects of relief distribution. For example, temporal equity that is equity related to the time required to deliver the relief commodities at each demand node, or social equity that ensures equitable relief distribution across different populations in the study area. This would greatly benefit and improve the overall equitable relief distribution across the affected population of a region.

In addition, natural disasters like earthquakes are unpredictable and the extent of damage to the infrastructure and the number affected people are highly uncertain. In this study, a deterministic mathematical formulation is considered that does not explicitly consider the uncertainty associated with demand/supply values, travel times, and available ground and aerial modes of transportation. To address this, the proposed deterministic model can be extended to a stochastic model by incorporating the uncertainty in some of the model parameters such as the demand and supply values and the travel times. A stochastic approach would allow understanding the impact of uncertainty for these parameters on the design and operation of the relief distribution network as the expected values of unmet demand and total travel time are minimized simultaneously.

In addition to the previously mentioned limitations, there are several potential avenues for future research that could enhance the applicability and scalability of the proposed model.

One such direction could be evaluating problem instances with a larger number of DCs and demand nodes, thereby capturing a more comprehensive representation of real-world scenarios. By considering additional DCs and demand nodes, the model would provide a more nuanced understanding of the relief distribution design and operation, and allow for developing more insights for future decision-making.

Furthermore, the inclusion of vehicle routing in the model would significantly enhance its practicality. By incorporating vehicle routing, the model would not only determine the optimal allocation of vehicles but also devise efficient routes for distributing the relief commodities to the various affected areas in every period of the planning horizon. This would ensure that the available vehicles are utilized optimally and that the relief supplies reach the affected populations in a timely and cost-effective manner. This would be particularly important for situations in which there is a limited number of vehicles available for the distribution.

As the problem size and complexity increase, heuristic methods could be developed and implemented to solve the optimization problem efficiently. Heuristics such as metaheuristic algorithms (e.g., NSGA II) or local search algorithms could be applied to find near-optimal solutions within reasonable computational times. These methods could potentially overcome the computational challenges associated with larger instances of the problem and provide effective solutions that approximate the optimal outcomes.

These advancements would enable a more comprehensive and practical approach to the relief distribution optimization scenario discussed in this thesis, providing decision-makers with valuable insights and tools to improve the efficiency and effectiveness of their disaster response planning.

References

Afshar, A., & Haghani, A. (2012). Modeling integrated supply chain logistics in real-time large-scale disaster relief operations. *Socio-economic Planning Sciences*, *46*(4), 327–338. https://doi.org/10.1016/j.seps.2011.12.003

Anaya-Arenas, A. M., Ruiz, A., & Coelho, L. C. (2018). Importance of fairness in humanitarian relief distribution. *Production Planning & Control*, *29*(14), 1145–1157. https://doi.org/10.1080/09537287.2018.1542157

Balcik, B., & Smilowitz, K. (2020). Contributions to Humanitarian and Non-profit Operations: Equity Impacts on Modeling and Solution Approaches. In *Springer eBooks* (pp. 371–390). https://doi.org/10.1007/978-3-030-11866-2_16

Barbarosoğlu, G., & Arda, Y. (2004). A two-stage stochastic programming framework for transportation planning in disaster response. *Journal of the Operational Research Society*, *55*(1), 43–53. https://doi.org/10.1057/palgrave.jors.2601652

Boonmee, C., Arimura, M., & Asada, T. (2017). Facility location optimization model for emergency humanitarian logistics. *International Journal of Disaster Risk Reduction*, *24*, 485–498. https://doi.org/10.1016/j.ijdrr.2017.01.017

Buylova, A., Chen, C., Cramer, L. A., Wang, H., & Cox, D. J. (2020a). Household risk perceptions and evacuation intentions in earthquake and tsunami in a Cascadia Subduction Zone. *International Journal of Disaster Risk Reduction*, *44*, 101442. https://doi.org/10.1016/j.ijdrr.2019.101442

Buylova, A., Chen, C., Cramer, L. A., Wang, H., & Cox, D. J. (2020b). Household risk perceptions and evacuation intentions in earthquake and tsunami in a Cascadia Subduction Zone. *International Journal of Disaster Risk Reduction*, *44*, 101442. https://doi.org/10.1016/j.ijdrr.2019.101442

Buylova, A., Chen, C., Cramer, L. A., Wang, H., & Cox, D. J. (2020c). Household risk perceptions and evacuation intentions in earthquake and tsunami in a Cascadia Subduction Zone. *International Journal of Disaster Risk Reduction*, *44*, 101442. https://doi.org/10.1016/j.ijdrr.2019.101442

Cao, C., Li, C., Yang, Q., Liu, Y., & Qu, T. (2018). A novel multi-objective programming model of relief distribution for sustainable disaster supply chain in large-scale natural disasters. *Journal of Cleaner Production*, *174*, 1422–1435. https://doi.org/10.1016/j.jclepro.2017.11.037

CDC Works 24/7. (2023, June 22). Center for Disease Control and Prevention. https://cdc.gov/

Chapman, A. G., & Mitchell, J. C. (2018). A fair division approach to humanitarian logistics inspired by conditional value-at-risk. *Annals of Operations Research*, *262*(1), 133–151. https://doi.org/10.1007/s10479-016-2322-1

Condeixa, L. D., Leiras, A., Oliveira, F., & De Brito, I., Junior. (2017). Disaster relief supply pre-positioning optimization: A risk analysis via shortage mitigation. *International Journal of Disaster Risk Reduction*, *25*, 238–247. https://doi.org/10.1016/j.ijdrr.2017.09.007

Ershadi, M. J., & Shemirani, H. S. (2021). A multi-objective optimization model for logistic planning in the crisis response phase. *Journal of Humanitarian Logistics and Supply Chain Management*, *12*(1), 30–53. https://doi.org/10.1108/jhlscm-11-2020-0108

Ertem, M. A., Akdogan, M. A., & Kahya, M. (2022). Intermodal transportation in humanitarian logistics with an application to a Turkish network using retrospective analysis. *International Journal of Disaster Risk Reduction*, *72*, 102828. https://doi.org/10.1016/j.ijdrr.2022.102828

FEMA.gov. (2020). HAZUS-MH MR4 *user manual, multi-hazard loss estimation methodology earthquake model*. https://www.fema.gov/

Free Map Tools. (2017). https://www.freemaptools.com/

Galkina, A., & Grafeeva, N. (2019). Machine Learning Methods for Earthquake Prediction: a Survey. *ResearchGate*. https://www.researchgate.net/publication/333774922

Gao, X., Jin, X., Zheng, P., & Wang, P. (2021). Multi-modal transportation planning for multi-commodity rebalancing under uncertainty in humanitarian logistics. *Advanced Engineering Informatics*, *47*, 101223. https://doi.org/10.1016/j.aei.2020.101223

Ghasemi, P., Khalili-Damghani, K., Hafezalkotob, A., & Raissi, S. (2019). Uncertain multi-objective multi-commodity multi-period multi-vehicle location-allocation model for earthquake evacuation planning. *Applied Mathematics and Computation*, *350*, 105–132. https://doi.org/10.1016/j.amc.2018.12.061

Gutjahr, W. J., & Fischer, S. (2018). Equity and deprivation costs in humanitarian logistics. *European Journal of Operational Research*, *270*(1), 185–197. https://doi.org/10.1016/j.ejor.2018.03.019

Hernández-Leandro, N. A., Ibarra-Rojas, O. J., & Camacho-Vallejo, J. (2022). A bi-objective humanitarian logistics model considering equity in the affected zones: application to a recent earthquake in Mexico. *Rairo-operations Research*. https://doi.org/10.1051/ro/2022067

Huang, K., Jiang, Y., Yuan, Y., & Zhao, L. (2015). Modeling multiple humanitarian objectives in emergency response to large-scale disasters. *Transportation Research Part E-logistics and Transportation Review*, *75*, 1–17. https://doi.org/10.1016/j.tre.2014.11.007

Huang, K., & Rafiei, R. (2019). Equitable last mile distribution in emergency response. *Computers & Industrial Engineering*, *127*, 887–900. https://doi.org/10.1016/j.cie.2018.11.025

Hwang, C., & Yoon, K. (1981). Methods for Multiple Attribute Decision Making. In *Lecture Notes in Economics and Mathematical Systems* (pp. 58–191). Springer Science+Business Media. https://doi.org/10.1007/978-3-642-48318-9_3

Kiremidjian, A., Moore, J., Fan, Y. Y., Yazlali, O., Basoz, N., & Williams, M. (2007). Seismic Risk Assessment of Transportation Network Systems. *Journal of Earthquake Engineering*, *11*(3), 371–382. https://doi.org/10.1080/13632460701285277

Knudson, M. P., Ballantyne, D. L., Stuhr, M., & Damewood, M. (2014). The Oregon Resilience Plan for Water and Wastewater Systems. In *Pipelines 2014*. https://doi.org/10.1061/9780784413692.201

Liu, C., Kou, G., Peng, Y., & Alsaadi, F. E. (2019). Location-Routing Problem for Relief Distribution in the Early Post-Earthquake Stage from the Perspective of Fairness. *Sustainability*, *11*(12), 3420. https://doi.org/10.3390/su11123420

Maghfiroh, M. F. N., & Hanaoka, S. (2020). Multi-modal relief distribution model for disaster response operations. *Progress in Disaster Science*, *6*, 100095. https://doi.org/10.1016/j.pdisas.2020.100095

Mahapatra, M. S., & Mahanty, B. (2022). Equitable and effective distribution under capacity constraint and limited budget for capacity augmentation. *Computers & Industrial Engineering*, *172*, 108649. https://doi.org/10.1016/j.cie.2022.108649

Mohammadi, S., Darestani, S. A., Vahdani, B., & Alinezhad, A. (2020). A robust neutrosophic fuzzy-based approach to integrate reliable facility location and routing decisions for disaster relief under fairness and aftershocks concerns. *Computers & Industrial Engineering*, *148*, 106734. https://doi.org/10.1016/j.cie.2020.106734

Nedjati, A., & Vizvári, B. (2015). Post-earthquake response by small UAV helicopters. *Natural Hazards*, *80*(3), 1669–1688. https://doi.org/10.1007/s11069-015-2046-6

Noyan, N., Balcik, B., & Atakan, S. (2016). A Stochastic Optimization Model for Designing Last Mile Relief Networks. *Transportation Science*, *50*(3), 1092–1113. https://doi.org/10.1287/trsc.2015.0621

Noyan, N., & Kahvecioğlu, G. (2018). Stochastic last mile relief network design with resource reallocation. *OR Spectrum*, *40*(1), 187–231. https://doi.org/10.1007/s00291-017-0498-7

Oregon Resilience Plan. (2013). *Reducing Risk and Improving Recovery for the Next Cascadia Earthquake and Tsunami.* https://www.oregon.gov

Oregon Department of Emergency Management : Cascadia Subduction Zone : Hazards and Preparedness : State of Oregon. Cascadia Subduction Zone : Oregon Department of Emergency Management https://www.oregon.gov/oem/hazardsprep/pages/cascadia-subduction-zone.aspx

Precision Nutrition. (2023, June 19). *Nutrition Certification, Coaching & Courses | Precision Nutrition*. https://precisionnutrition.com/

Ransikarbum, K., & Mason, S. J. (2016). Multiple-objective analysis of integrated relief supply and network restoration in humanitarian logistics operations. *International Journal of Production Research*, *54*(1), 49–68. https://doi.org/10.1080/00207543.2014.977458

Rao, S. S. (2009). *Engineering Optimization: Theory and Practice*. John Wiley & Sons.

Salvadó, L. L., Lauras, M., & Comes, T. (2017). Sustainable performance measurement for humanitarian supply chain operations. In *HAL (Le Centre pour la Communication Scientifique Directe)*. French National Centre for Scientific Research. https://hal-mines-albi.archives-ouvertes.fr/hal-01686623

Shavarani, S. M. (2019). Multi-level facility location-allocation problem for post-disaster humanitarian relief distribution. *Journal of Humanitarian Logistics and Supply Chain Management*, *9*(1), 70–81. https://doi.org/10.1108/jhlscm-05-2018-0036

StorageArea: Find Cheap Self Storage Units Near You. (2023). StorageArea. https://storagearea.com/

Svenson, J. E., O'Connor, J. E., & Lindsay, M. B. (2006). Is air transport faster? A comparison of air versus ground transport times for interfacility transfers in a regional referral system. *Air Medical Journal*, *25*(4), 170–172. https://doi.org/10.1016/j.amj.2006.04.003

Tzeng, G., Cheng, H., & Huang, T. (2007). Multi-objective optimal planning for designing relief delivery systems. *Transportation Research Part E-logistics and Transportation Review*, *43*(6), 673–686. https://doi.org/10.1016/j.tre.2006.10.012

United States Geological Survey. (2020). *ShakeMap*. https://earthquake.usgs.gov/data/shakemap/

USDA Foods Disaster Manual, (2021). https://usda.gov

Veysmoradi, D., Vahdani, B., Sartangi, M. F., & Mousavi, S. M. (2017). Multi-objective open location-routing model for relief distribution networks with split delivery and multi-mode transportation under uncertainty. *Scientia Iranica*, *0*(0), 0. https://doi.org/10.24200/sci.2017.4572

Volgenant, A. (2002). Solving some lexicographic multi-objective combinatorial problems. *European Journal of Operational Research*, *139*(3), 578–584. https://doi.org/10.1016/s0377-2217(01)00214-4

7 Standard Retail Spaces in a Transforming Industry. (2018). vts.com.

Wang, S., & Sun, B. (2023). Model of multi-period emergency material allocation for large-scale sudden natural disasters in humanitarian logistics: Efficiency, effectiveness and equity. *https://doi.org/10.1016/j.ijdrr.2023.103530*, *85*, 103530. https://doi.org/10.1016/j.ijdrr.2023.103530

Wang, Z., & Rangaiah, G. P. (2017). Application and Analysis of Methods for Selecting an Optimal Solution from the Pareto-Optimal Front obtained by Multiobjective Optimization. *Industrial & Engineering Chemistry Research*, *56*(2), 560–574. https://doi.org/10.1021/acs.iecr.6b03453

APPENDICES

Appendix A – DEMAND ESTIMATES FOR SCENARIO 3 AND SCENARIO 4

The demand for each demand node is estimated based on the number of displaced people and number of people needing short-term shelter provided by the Hazus-MH software. We do not include the number of casualties provided by the software, since the casualties include injured people requiring medical attention at a different location and deadly victims of the earthquake event. Based on the number of affected people at each demand node, the demand is estimated in terms of total weight of food, water or first aid required, as described in Section 5.2.1. Table A.1 presents the demand estimates for Scenario 3 and Scenario 4 for a M8.0 CSZ earthquake.

Table A.1 *Demand Estimates for M8.0 CSZ Earthquake (in hundreds of pounds)*

Demand Nodes	Commodity	Period 1	Period 2	Period 3
Beaverton	Food	1786	1969	1620
	Water	2381	2256	2717
	Medicine	297	317	264
Portland	Food	2514	2853	2741
	Water	3352	3385	3065
	Medicine	419	368	398
Astoria	Food	185	201	165
	Water	247	280	263
	Medicine	31	30	29
St Helens	Food	84	91	94
	Water	112	120	111
	Medicine	14	15	14
McMinnville	Food	280	291	313
	Water	383	412	372
	Medicine	48	52	54

Salem	Food	890	939	1009
	Water	1196	1302	1137
	Medicine	149	162	164
Dallas	Food	250	285	268
	Water	338	295	380
	Medicine	42	41	36
Newport	Food	170	157	165
	Water	227	227	222
	Medicine	28	27	31
Albany	Food	267	267	304
	Water	356	355	375
	Medicine	44	49	44
Corvallis	Food	395	442	350
	Water	527	557	596
	Medicine	66	66	69
Eugene	Food	1148	1051	1104
	Water	1531	1562	1564
	Medicine	191	207	202
Winston	Food	421	448	439
	Water	562	615	616
	Medicine	70	71	61
Medford	Food	410	447	462
	Water	547	493	546
	Medicine	68	69	75
Grants Pass	Food	172	176	160
	Water	229	224	250
	Medicine	28	26	29

Appendix B – TOPSIS RESULTS

In this section, we present the complete results for the TOPSIS solution for Scenario1. Table B.1 includes the DC-demand node pairs along with the quantity of relief commodity distributed via ground/air. Table B.2 summarizes the total unmet demand for every demand node in each time period. Table B.3 illustrates the percentage of demand met for each commodity across all three periods, and finally Table B.4 displays the average demand met for every commodity in all three periods.

Table B.1 *Relief Commodities Distributed from DCs to Demand Node via Ground/Air (in hundreds of pounds)*

Period	DC	Demand Node	Commodity	Ground	Air
1	SANDY	BEAVERTON	MEDICINE	0	221
1	SANDY	PORTLAND	FOOD	1428	0
1	SANDY	PORTLAND	WATER	0	1902
1	SANDY	ST HELENS	MEDICINE	0	13
1	OREGON CITY	PORTLAND	MEDICINE	135	0
1	OREGON CITY	ASTORIA	FOOD	190	0
1	OREGON CITY	ASTORIA	WATER	0	219
1	OREGON CITY	ASTORIA	MEDICINE	28	0
1	OREGON CITY	ST HELENS	FOOD	65	0
1	OREGON CITY	ST HELENS	WATER	103	0
1	OREGON CITY	MCMINNVILLE	FOOD	0	323
1	OREGON CITY	MCMINNVILLE	WATER	419	0
1	OREGON CITY	MCMINNVILLE	MEDICINE	0	41
1	OREGON CITY	SALEM	FOOD	0	833
1	OREGON CITY	SALEM	WATER	0	852
1	OREGON CITY	DALLAS	WATER	0	340
1	OREGON CITY	DALLAS	MEDICINE	34	0

1	ROSEBURG	EUGENE	FOOD	421	0
1	ROSEBURG	EUGENE	WATER	469	0
1	ROSEBURG	WINSTON	FOOD	0	515
1	ROSEBURG	WINSTON	WATER	697	0
1	ROSEBURG	WINSTON	MEDICINE	85	0
1	ROSEBURG	MEDFORD	FOOD	0	361
1	ROSEBURG	MEDFORD	WATER	0	511
1	ROSEBURG	MEDFORD	MEDICINE	63	0
1	ROSEBURG	GRANTS PASS	FOOD	0	155
1	ROSEBURG	GRANTS PASS	WATER	207	0
1	ROSEBURG	GRANTS PASS	MEDICINE	0	33
1	MADRAS	PORTLAND	FOOD	1442	0
1	MADRAS	PORTLAND	WATER	1932	0
1	MADRAS	PORTLAND	MEDICINE	232	0
1	BEND	BEAVERTON	FOOD	0	1455
1	BEND	BEAVERTON	WATER	1870	0
1	BEND	EUGENE	MEDICINE	0	186
1	JUNCTION CITY	SALEM	MEDICINE	115	0
1	JUNCTION CITY	DALLAS	FOOD	196	0
1	JUNCTION CITY	NEWPORT	FOOD	0	163
1	JUNCTION CITY	NEWPORT	WATER	216	0
1	JUNCTION CITY	NEWPORT	MEDICINE	0	35
1	JUNCTION CITY	ALBANY	FOOD	198	0
1	JUNCTION CITY	ALBANY	WATER	261	0
1	JUNCTION CITY	ALBANY	MEDICINE	39	0
1	JUNCTION CITY	CORVALLIS	FOOD	396	0
1	JUNCTION CITY	CORVALLIS	WATER	0	406
1	JUNCTION CITY	CORVALLIS	MEDICINE	2	51
1	JUNCTION CITY	EUGENE	FOOD	0	498
1	JUNCTION CITY	EUGENE	WATER	0	1023

2	OREGON CITY	PORTLAND	MEDICINE	0	74
2	OREGON CITY	ASTORIA	FOOD	0	263
2	OREGON CITY	ASTORIA	WATER	0	323
2	OREGON CITY	ASTORIA	MEDICINE	0	34
2	OREGON CITY	ST HELENS	FOOD	0	80
2	OREGON CITY	ST HELENS	WATER	0	128
2	OREGON CITY	MCMINNVILLE	FOOD	338	0
2	OREGON CITY	MCMINNVILLE	WATER	398	0
2	OREGON CITY	MCMINNVILLE	MEDICINE	0	44
2	OREGON CITY	SALEM	FOOD	912	4
2	OREGON CITY	SALEM	WATER	0	934
2	OREGON CITY	SALEM	MEDICINE	0	120
2	OREGON CITY	DALLAS	WATER	351	0
2	ROSEBURG	EUGENE	FOOD	1	538
2	ROSEBURG	EUGENE	WATER	519	0
2	ROSEBURG	WINSTON	FOOD	520	0
2	ROSEBURG	WINSTON	WATER	0	846
2	ROSEBURG	WINSTON	MEDICINE	0	72
2	ROSEBURG	MEDFORD	FOOD	399	0
2	ROSEBURG	MEDFORD	WATER	0	476
2	ROSEBURG	MEDFORD	MEDICINE	0	65
2	ROSEBURG	GRANTS PASS	FOOD	203	0
2	ROSEBURG	GRANTS PASS	WATER	0	232
2	ROSBURG	GRANTS PASS	MEDICINE	36	0
2	MADRAS	PORTLAND	FOOD	669	893
2	MADRAS	PORTLAND	WATER	0	2107
2	MADRAS	PORTLAND	MEDICINE	270	0
2	BEND	BEAVERTON	WATER	2039	0
2	BEND	BEAVERTON	MEDICINE	0	0
2	BEND	PORTLAND	FOOD	1543	0

2	JUNCTION CITY	DALLAS	FOOD	247	0
2	JUNCTION CITY	DALLAS	WATER	0	0
2	JUNCTION CITY	DALLAS	MEDICINE	30	0
2	JUNCTION CITY	NEWPORT	FOOD	0	179
2	JUNCTION CITY	NEWPORT	WATER	0	299
2	JUNCTION CITY	NEWPORT	MEDICINE	25	0
2	JUNCTION CITY	ALBANY	FOOD	254	0
2	JUNCTION CITY	ALBANY	WATER	300	0
2	JUNCTION CITY	ALBANY	MEDICINE	0	32
2	JUNCTION CITY	CORVALLIS	FOOD	0	321
2	JUNCTION CITY	CORVALLIS	WATER	0	477
2	JUNCTION CITY	CORVALLIS	MEDICINE	0	49
2	JUNCTION CITY	EUGENE	FOOD	0	539
2	JUNCTION CITY	EUGENE	WATER	1149	0
2	JUNCTION CITY	EUGENE	MEDICINE	127	0
3	SANDY	PORTLAND	FOOD	1582	0
3	SANDY	PORTLAND	WATER	0	2042
3	SANDY	PORTLAND	MEDICINE	275	0
3	SANDY	ASTORIA	MEDICINE	0	0
3	SANDY	ST HELENS	FOOD	0	111
3	OREGON CITY	PORTLAND	MEDICINE	107	0
3	OREGON CITY	ASTORIA	FOOD	238	0
3	OREGON CITY	ASTORIA	WATER	0	288
3	OREGON CITY	ASTORIA	MEDICINE	27	0
3	OREGON CITY	ST HELENS	FOOD	0	0
3	OREGON CITY	ST HELENS	WATER	95	0
3	OREGON CITY	ST HELENS	MEDICINE	12	0
3	OREGON CITY	MCMINNVILLE	FOOD	0	273
3	OREGON CITY	MCMINNVILLE	WATER	0	460
3	OREGON CITY	MCMINNVILLE	MEDICINE	47	0

3	OREGON CITY	SALEM	FOOD	0	805
3	OREGON CITY	SALEM	WATER	0	1097
3	OREGON CITY	SALEM	MEDICINE	0	0
3	OREGON CITY	DALLAS	FOOD	0	289
3	OREGON CITY	DALLAS	WATER	0	339
3	OREGON CITY	DALLAS	MEDICINE	0	31
3	OREGON CITY	ALBANY	MEDICINE	35	0
3	ROSEBURG	EUGENE	FOOD	477	0
3	ROSEBURG	EUGENE	WATER	488	3
3	ROSEBURG	EUGENE	MEDICINE	0	0
3	ROSEBURG	WINSTON	FOOD	481	0
3	ROSEBURG	WINSTON	WATER	829	0
3	ROSEBURG	WINSTON	MEDICINE	89	0
3	ROSEBURG	MEDFORD	FOOD	417	0
3	ROSEBURG	MEDFORD	WATER	0	483
3	ROSEBURG	MEDFORD	MEDICINE	73	0
3	ROSEBURG	GRANTS PASS	FOOD	239	0
3	ROSEBURG	GRANTS PASS	WATER	0	216
3	ROSEBURG	GRANTS PASS	MEDICINE	0	35
3	MADRAS	BEAVERTON	MEDICINE	0	270
3	MADRAS	PORTLAND	FOOD	876	720
3	MADRAS	PORTLAND	WATER	0	2280
3	BEND	BEAVERTON	FOOD	0	1724
3	BEND	BEAVERTON	WATER	790	1276
3	BEND	SALEM	MEDICINE	0	135
3	JUNCTION CITY	NEWPORT	FOOD	251	0
3	JUNCTION CITY	NEWPORT	WATER	0	227
3	JUNCTION CITY	NEWPORT	MEDICINE	0	29
3	JUNCTION CITY	ALBANY	FOOD	303	0
3	JUNCTION CITY	ALBANY	WATER	309	0

3	JUNCTION CITY	ALBANY	MEDICINE	0	0
3	JUNCTION CITY	CORVALLIS	FOOD	0	421
3	JUNCTION CITY	CORVALLIS	WATER	414	0
3	JUNCTION CITY	CORVALLIS	MEDICINE	71	0
3	JUNCTION CITY	EUGENE	FOOD	642	0
3	JUNCTION CITY	EUGENE	WATER	3	1159
3	JUNCTION CITY	EUGENE	MEDICINE	158	0

Table B.2 *Unmet Demand of Each Commodity during Three Periods (in hundreds of pounds)*

Period	Demand Node	Commodity	Unmet Demand
1	BEAVERTON	FOOD	495
1	BEAVERTON	WATER	730
1	BEAVERTON	MEDICINE	104
1	PORTLAND	FOOD	510
1	PORTLAND	WATER	676
1	PORTLAND	MEDICINE	197
1	ASTORIA	FOOD	62
1	ASTORIA	WATER	117
1	ASTORIA	MEDICINE	14
1	ST HELENS	FOOD	35
1	ST HELENS	WATER	27
1	ST HELENS	MEDICINE	3
1	MCMINNVILLE	FOOD	57
1	MCMINNVILLE	WATER	87
1	MCMINNVILLE	MEDICINE	22
1	SALEM	FOOD	147
1	SALEM	WATER	458
1	SALEM	MEDICINE	49
1	DALLAS	FOOD	104
1	DALLAS	WATER	60
1	DALLAS	MEDICINE	16
1	NEWPORT	FOOD	87
1	NEWPORT	WATER	114
1	NEWPORT	MEDICINE	7
1	ALBANY	FOOD	102
1	ALBANY	WATER	140
1	ALBANY	MEDICINE	11

1	CORVALLIS	FOOD	70
1	CORVALLIS	WATER	214
1	CORVALLIS	MEDICINE	24
1	EUGENE	FOOD	391
1	EUGENE	WATER	264
1	EUGENE	MEDICINE	34
1	WINSTON	FOOD	105
1	WINSTON	WATER	123
1	WINSTON	MEDICINE	15
1	MEDFORD	FOOD	89
1	MEDFORD	WATER	91
1	MEDFORD	MEDICINE	12
1	GRANTS PASS	FOOD	83
1	GRANTS PASS	WATER	110
1	GRANTS PASS	MEDICINE	7
2	BEAVERTON	FOOD	509
2	BEAVERTON	WATER	139
2	BEAVERTON	MEDICINE	54
2	PORTLAND	FOOD	227
2	PORTLAND	WATER	413
2	PORTLAND	MEDICINE	185
2	ASTORIA	FOOD	11
2	ASTORIA	WATER	17
2	ASTORIA	MEDICINE	13
2	ST HELENS	FOOD	24
2	ST HELENS	WATER	7
2	ST HELENS	MEDICINE	4
2	MCMINNVILLE	FOOD	14
2	MCMINNVILLE	WATER	123
2	MCMINNVILLE	MEDICINE	23

2	SALEM	FOOD	46
2	SALEM	WATER	308
2	SALEM	MEDICINE	64
2	DALLAS	FOOD	77
2	DALLAS	WATER	23
2	DALLAS	MEDICINE	16
2	NEWPORT	FOOD	56
2	NEWPORT	WATER	63
2	NEWPORT	MEDICINE	13
2	ALBANY	FOOD	79
2	ALBANY	WATER	99
2	ALBANY	MEDICINE	17
2	CORVALLIS	FOOD	82
2	CORVALLIS	WATER	157
2	CORVALLIS	MEDICINE	26
2	EUGENE	FOOD	46
2	EUGENE	WATER	86
2	EUGENE	MEDICINE	67
2	WINSTON	FOOD	21
2	WINSTON	WATER	53
2	WINSTON	MEDICINE	18
2	MEDFORD	FOOD	17
2	MEDFORD	WATER	157
2	MEDFORD	MEDICINE	16
2	GRANTS PASS	FOOD	63
2	GRANTS PASS	WATER	76
2	GRANTS PASS	MEDICINE	9
3	BEAVERTON	FOOD	23
3	BEAVERTON	WATER	755
3	BEAVERTON	MEDICINE	68

3	PORTLAND	FOOD	573
3	PORTLAND	WATER	681
3	PORTLAND	MEDICINE	198
3	ASTORIA	FOOD	32
3	ASTORIA	WATER	31
3	ASTORIA	MEDICINE	13
3	ST HELENS	FOOD	2
3	ST HELENS	WATER	38
3	ST HELENS	MEDICINE	4
3	MCMINNVILLE	FOOD	73
3	MCMINNVILLE	WATER	46
3	MCMINNVILLE	MEDICINE	22
3	SALEM	FOOD	195
3	SALEM	WATER	109
3	SALEM	MEDICINE	23
3	DALLAS	FOOD	4
3	DALLAS	WATER	56
3	DALLAS	MEDICINE	16
3	NEWPORT	FOOD	4
3	NEWPORT	WATER	92
3	NEWPORT	MEDICINE	7
3	ALBANY	FOOD	5
3	ALBANY	WATER	126
3	ALBANY	MEDICINE	17
3	CORVALLIS	FOOD	114
3	CORVALLIS	WATER	166
3	CORVALLIS	MEDICINE	17
3	EUGENE	FOOD	303
3	EUGENE	WATER	170
3	EUGENE	MEDICINE	72

3	WINSTON	FOOD	130
3	WINSTON	WATER	82
3	WINSTON	MEDICINE	15
3	MEDFORD	FOOD	88
3	MEDFORD	WATER	131
3	MEDFORD	MEDICINE	13
3	GRANTS PASS	FOOD	4
3	GRANTS PASS	WATER	86
3	GRANTS PASS	MEDICINE	6

Table B.3. *Percentage of Demand Met of Each Commodity during Three Periods*

Period	Demand Node	Commodity	% of Demand Met
1	BEAVERTON	FOOD	75%
1	PORTLAND	FOOD	85%
1	ASTORIA	FOOD	75%
1	ST HELENS	FOOD	65%
1	MCMINNVILLE	FOOD	85%
1	SALEM	FOOD	85%
1	DALLAS	FOOD	65%
1	NEWPORT	FOOD	65%
1	ALBANY	FOOD	66%
1	CORVALLIS	FOOD	85%
1	EUGENE	FOOD	70%
1	WINSTON	FOOD	83%
1	MEDFORD	FOOD	80%
1	GRANTS PASS	FOOD	65%
1	BEAVERTON	WATER	72%
1	PORTLAND	WATER	85%
1	ASTORIA	WATER	65%
1	ST HELENS	WATER	79%
1	MCMINNVILLE	WATER	83%
1	SALEM	WATER	65%
1	DALLAS	WATER	85%
1	NEWPORT	WATER	65%
1	ALBANY	WATER	65%
1	CORVALLIS	WATER	65%
1	EUGENE	WATER	85%
1	WINSTON	WATER	85%
1	MEDFORD	WATER	85%
1	GRANTS PASS	WATER	65%

1	BEAVERTON	MEDICINE	68%
1	PORTLAND	MEDICINE	65%
1	ASTORIA	MEDICINE	67%
1	ST HELENS	MEDICINE	81%
1	MCMINNVILLE	MEDICINE	65%
1	SALEM	MEDICINE	70%
1	DALLAS	MEDICINE	68%
1	NEWPORT	MEDICINE	83%
1	ALBANY	MEDICINE	78%
1	CORVALLIS	MEDICINE	69%
1	EUGENE	MEDICINE	85%
1	WINSTON	MEDICINE	85%
1	MEDFORD	MEDICINE	84%
1	GRANTS PASS	MEDICINE	83%
2	BEAVERTON	FOOD	76%
2	PORTLAND	FOOD	93%
2	ASTORIA	FOOD	96%
2	ST HELENS	FOOD	77%
2	MCMINNVILLE	FOOD	96%
2	SALEM	FOOD	95%
2	DALLAS	FOOD	76%
2	NEWPORT	FOOD	76%
2	ALBANY	FOOD	76%
2	CORVALLIS	FOOD	80%
2	EUGENE	FOOD	96%
2	WINSTON	FOOD	96%
2	MEDFORD	FOOD	96%
2	GRANTS PASS	FOOD	76%
2	BEAVERTON	WATER	95%
2	PORTLAND	WATER	89%

2	ASTORIA	WATER	95%
2	ST HELENS	WATER	95%
2	MCMINNVILLE	WATER	76%
2	SALEM	WATER	75%
2	DALLAS	WATER	94%
2	NEWPORT	WATER	83%
2	ALBANY	WATER	75%
2	CORVALLIS	WATER	75%
2	EUGENE	WATER	95%
2	WINSTON	WATER	94%
2	MEDFORD	WATER	75%
2	GRANTS PASS	WATER	75%
2	BEAVERTON	MEDICINE	81%
2	PORTLAND	MEDICINE	65%
2	ASTORIA	MEDICINE	72%
2	ST HELENS	MEDICINE	76%
2	MCMINNVILLE	MEDICINE	66%
2	SALEM	MEDICINE	65%
2	DALLAS	MEDICINE	65%
2	NEWPORT	MEDICINE	66%
2	ALBANY	MEDICINE	65%
2	CORVALLIS	MEDICINE	65%
2	EUGENE	MEDICINE	65%
2	WINSTON	MEDICINE	80%
2	MEDFORD	MEDICINE	80%
2	GRANTS PASS	MEDICINE	80%
3	BEAVERTON	FOOD	99%
3	PORTLAND	FOOD	85%
3	ASTORIA	FOOD	88%
3	ST HELENS	FOOD	98%

3	MCMINNVILLE	FOOD	79%
3	SALEM	FOOD	81%
3	DALLAS	FOOD	99%
3	NEWPORT	FOOD	98%
3	ALBANY	FOOD	98%
3	CORVALLIS	FOOD	79%
3	EUGENE	FOOD	79%
3	WINSTON	FOOD	79%
3	MEDFORD	FOOD	83%
3	GRANTS PASS	FOOD	98%
3	BEAVERTON	WATER	73%
3	PORTLAND	WATER	86%
3	ASTORIA	WATER	90%
3	ST HELENS	WATER	71%
3	MCMINNVILLE	WATER	91%
3	SALEM	WATER	91%
3	DALLAS	WATER	86%
3	NEWPORT	WATER	71%
3	ALBANY	WATER	71%
3	CORVALLIS	WATER	71%
3	EUGENE	WATER	91%
3	WINSTON	WATER	91%
3	MEDFORD	WATER	79%
3	GRANTS PASS	WATER	72%
3	BEAVERTON	MEDICINE	80%
3	PORTLAND	MEDICINE	66%
3	ASTORIA	MEDICINE	68%
3	ST HELENS	MEDICINE	75%
3	MCMINNVILLE	MEDICINE	68%
3	SALEM	MEDICINE	85%

3	DALLAS	MEDICINE	66%
3	NEWPORT	MEDICINE	81%
3	ALBANY	MEDICINE	67%
3	CORVALLIS	MEDICINE	81%
3	EUGENE	MEDICINE	69%
3	WINSTON	MEDICINE	86%
3	MEDFORD	MEDICINE	85%
3	GRANTS PASS	MEDICINE	85%

Table B.4 *Average Demand Met of Every Commodity during Three Periods*

Period	Commodity	Average % of Demand Met
1	FOOD	75%
1	WATER	75%
1	MEDICINE	75%
2	FOOD	86%
2	WATER	85%
2	MEDICINE	71%
3	FOOD	89%
3	WATER	81%
3	MEDICINE	76%